ФИЗИКА ЭЛЕМЕНТАРНЫХ ЧАСТИЦ И АТОМНОГО ЯДРА
2016. Т. 47. ВЫП. 5

WEAK BOUND STATE WITH THE NONZERO CHARGE DENSITY AS THE LHC 126.5 GeV STATE

*J. Syska**

Department of Field Theory and Particle Physics, Institute of Physics,

University of Silesia, Katowice, Poland

*E-mail: jacek.syska@us.edu.pl

ФИЗИКА ЭЛЕМЕНТАРНЫХ ЧАСТИЦ И АТОМНОГО ЯДРА
2016. Т. 47. ВЫП. 5

WEAK BOUND STATE WITH THE NONZERO CHARGE DENSITY AS THE LHC 126.5 GeV STATE

J. Syska[*]

Department of Field Theory and Particle Physics, Institute of Physics,

University of Silesia, Katowice, Poland

The self-consistent model of classical field interactions formulated as the counterpart of the quantum electroweak model leads to homogeneous boson ground state solutions in presence of nonzero extended fermionic charge density fluctuations. Two different types of electroweak configurations of fields are analyzed. The first one has nonzero electric and weak charge fluctuations. The second one is electrically uncharged but weakly charged. Both types of configurations have two physically interesting solutions which possess masses equal to 126.67 GeV at the value of the scalar fluctuation potential parameter λ equal to ~ 0.0652. The spin zero electrically uncharged droplet, formed as a result of the decay of the charged one, is interpreted as the ~ 126.5 GeV state found in the Large Hadron Collider (LHC) experiment. The other two configurations correspond to solutions with masses equal to 123.7 GeV and λ equal to ~ 0.0498, and thus the algebraic mean of the masses of two central solutions, i.e., 126.67 and 123.7 GeV, is equal to 125.185 GeV. The problem of a mass of this kind of droplets will be considered on the basis of the phenomenon of the screening of the fluctuation of charges. Their masses are found in the thin wall approximation.

В качестве аналога квантовой электрослабой модели сформулирована самосогласованная модель взаимодействий классических полей, которая приводит к однородным решениям для бозонов в основном состоянии в присутствии ненулевых флуктуаций протяженной фермионной заряженной плотности. Рассмотрены две разные электрослабые конфигурации полей. Первая содержит ненулевые флуктуации электрического и слабого зарядов. Вторая является электрически нейтральной, но при этом ее слабый заряд не равен нулю. Обе конфигурации имеют два физически интересных решения с массой 126,67 ГэВ при значении параметра скалярного потенциала флуктуаций $\lambda \sim 0{,}0652$. Электрически нейтральная капля с нулевым спином, образующаяся в результате распада заряженной капли, интерпретируется как состояние с энергией $\sim 126{,}5$ ГэВ, обнаруженное в эксперименте на LHC. Две другие конфигурации соответствуют решениям с массами, равными первая — 123,7 ГэВ с $\lambda \sim 0{,}0498$ и вторая — алгебраическому среднему масс двух основных решений, а именно: 126,67 и 123,7 ГэВ, т. е. 125,185 ГэВ. Проблема масс капель такого типа рассматривается на

[*]E-mail: jacek.syska@us.edu.pl

основе явления экранирования флуктуаций заряда. Их массы вычисляются в приближении тонкой стены.

PACS: 21.60.Jz; 12.90.+b; 11.15.Kc

INTRODUCTION

In [1], the nonlinear self-consistent model of classical field interactions in the "classical counterpart of the electroweak Glashow–Salam–Weinberg" (CGSW) model was proposed. Homogeneous boson ground state solutions in this model in the presence of nonzero extended fermionic charge density fluctuations were reviewed and fully reinterpreted in order to make the theory with nonzero charge densities [2] coherent, as, unfortunately, the language in [2] uses both quantum field theory (QFT) concepts and the classical charge distributions. The model concerns the bound states of the matter of these fluctuations inside one droplet of fields. Because of the Pauli exclusion principle, only one or (for the sake of opposite projections [3–6] of the spin) two fermionic fluctuations in one droplet can occupy their lowest energy state. Unless other quantum numbers are assigned to these fluctuations, the consecutive fermionic fluctuations can eventually occupy their higher energy states. Concerning the phenomenon of the screening of the fluctuation of charges inside one droplet, we face the problem of the mass of this kind of droplet. The phenomenon of the gamma transparency of the electrically uncharged configuration of fields in the droplets in the reference to gamma bursts was previously pointed out in [7]. Below, the Schrödinger–Barut background of the model is given.

The analyzed CGSW model is not a modification of the quantum GSW model [8]. For instance, the configurations of fields are not the structures of QFT; most particularly, the ground state is not the QFT vacuum state. Hence, the argument against "a nonzero vacuum expectation value" is not relevant here, since in the body of the self-consistent field theory a structure like this does not exist at all. Unlike QFT, the self-consistent field theory (SCFT) deals with continuous charge densities and continuous charge density fluctuations as the basic concept [1, 9].

In order to present the idea of the ground field in a broader context, let us draw our attention to the Lagrangian density $\mathcal{L}$ of electromagnetism, which serves as an example for introducing the *ground field* notion in terms of the self-consistent theory only

$$\mathcal{L} = \bar{\Psi}(\gamma^\mu i\partial_\mu - m)\Psi + J^\mu A_\mu - \frac{1}{4} F_{\mu\nu} F^{\mu\nu},$$

where $J^\mu = -e\bar{\Psi}\gamma^\mu\Psi$ is the electron current density fluctuation and A_μ is the total electromagnetic field four-potential $A_\mu = A^e_\mu + A^s_\mu$, where the superscript e

stands for the external field and s stands for the self-field adjusted by the radiative reaction to suit the electron current and its fluctuations (see [10–15]). Then, in the minimum of the corresponding total Hamiltonian, the solution of the equation of motion for A^s_μ is called the *electromagnetic ground field*.

In this paper, the term *boson ground field* is used for the solution of equations of motion for a *boson field* in the ground state of the whole system of fields (fermion fluctuations, gauge bosons, scalar fluctuation) that are under consideration. This boson field is a self-field (or can be treated as one) when it is coupled to a source — "basic" field. In general, the term "basic" field means a wave function that is proper for a fermion (fluctuation), a scalar (fluctuation) or a dilatonic field [16, 17], and, although not in this paper, a charged or heavy boson (which in this case plays simultaneously the role of both the basic and ground fields).

The above-mentioned concept of a wave function and the Schrödinger wave equation is dominant in the nonrelativistic physics of atoms, molecules, and condensed matter [18]. In the relativistic quantum theory, this notion has been largely abandoned in favor of the second quantized perturbative Feynman graph approach, although the Dirac wave equation is still used for the approximation of some problems.

Barut and others extended Schrödinger's "charge density interpretation" of the wave function (e.g., the electron is the classical distribution of charge) to a "fully-fledged" relativistic theory. They successfully implemented this "natural (fields theory) interpretation" of the wave function with coupled Dirac and Maxwell equations (for characteristic boundary conditions) in many specific problems. But the "natural interpretation" of the wave function can be extended to the Klein–Gordon equation [16, 17] coupled to the Einstein field equations, thus being a rival for quantum gravity in its second quantization form. In the case of the QFT models, the second quantization approach is connected with the probabilistic interpretation that is inherent in the quantum theory, whereas the classical field theories and the "natural interpretation" of the wave function together with the self-field concept are in tune with the deterministic interpretation forming the relativistic SCFT.

Thus, depending on the model, the role of a self-field can be played by, e.g., the electromagnetic field [19–25], boson $W^+ - W^-$ and Z ground fields (as below in this paper) [1, 2], or by the gravitational field (metric tensor) $g_{\mu\nu}$ [16, 17]. The "basic" field that is proper for a particular matter source is the dominant factor in the existence of self-fields.

When the values of masses of fundamental fermionic, scalar, and bosonic fields have to be taken as the external parameters of the model, then in SCFT the basic fields are in fact interpreted as fluctuations [26–29] (of the total basic fields), and the self-fields are coupled to the fluctuations only. The conjecture is that if all fluctuations are identical to their total basic fields, then the solution

is fully self-consistent and the masses of all fields should appear as a result of the solution of the coupled partial differential equations that characterize the system [6, 30–35]. In [30–34], it was shown that the structural information of the system [5, 36, 37] is, in the case of the scalar field, proportional to its squared rest mass. The (observed) *structural information principle* put upon the system means that the analyticity requirement of the log-likelihood function of the system [5, 36] is used. The coupled set of self-consistently solved partial differential equations arises when the *variational information principle*, which minimizes the total physical information of the system [30–34, 36], is also put upon the system. In the analyses, the Rao–Fisher metricity of the statistical space [38] of the system is used [5, 39].

If only some of the fluctuations are identified with their total basic fields, then all masses of the fundamental fields remain among the parameters [39] that (at least at some value of the energy) are to be estimated from the experiment.

In accordance with the statement above, a model of bound states of fluctuations (index f) was constructed [1]. The new, electrically and/or weakly *charged physical configuration* lies in the minimum of the effective potential of the scalar field fluctuation φ_f at the value $\varphi_f = \delta$, which is calculated self-consistently from the Lagrangian of the CGSW model. In the model, the scalar field φ exists inside the droplet of the configuration of fields only. It is the only one (inside the droplet) to which its fluctuation $\varphi_f \equiv \varphi$ is possibly equivalent ("possibly", as this paper neither proves nor disproves it). In fact, it could be an effective one, e.g., the superposition of other fundamental fields or their fluctuations.

Thus, from now, the symbols φ_f, L_f, R_f denote the fluctuation of the scalar field and a doublet of left-handed or a singlet of right-handed fluctuations of fermionic fields, respectively, and not the global fields. In agreement with the above explanations of the self-consistent approach, fields in a doublet $L_f = \binom{\nu_{fL}}{\ell_{fL}}$ and a singlet $R_f = (\ell_{fR})$ are wave functions, where ℓ_f and ν_f signify a leptonic fluctuation ℓ and a fluctuation of its neutrino ν, respectively. Thus, fields in L_f and R_f are not connected with the interpretation of the corresponding full (global) charge density distributions for particles in the doublet L and singlet R, as it is for fields ruled by the original linear Dirac equation. Instead, they are associated with the distributions of the charge density *fluctuations* of fields in the doublet L and singlet R that are ruled by the coupled Dirac–Maxwell equations, similar to that found in Barut's case. Therefore, j^{μ}_{fY} and $j^{a\mu}_{f}$, $a = 1, 2, 3$, are the continuous matter current electroweak density fluctuations extended in space (and not operators of QFT with point-like charges). In order to simplify the calculations, the mass m_f of any fermionic fluctuation is neglected (see Eq. (82)).

In Sec. 1, the effective potential for the "boson ground fields induced by matter sources" configuration (hereafter, I will call it the bgfms configuration) and the general algebraic equations that follow from the field equations of motion

for the fields on the ground state inside the droplet are presented. They form the screening condition of the fluctuation of charges. Such quantities as the observed charge density fluctuations are also determined. In Sec. 2, the numerical results for the electrically and weakly charged bgfms (EWbgfms) configuration are presented along with the calculations of the mass of its droplet in the thin wall approximation. Section 3 is devoted to the analysis of the weakly charged bgfms (Wbgfms) configuration and its stability for the sake of both the weak charge density fluctuation and λ parameter (which is the parameter of the scalar fluctuation potential). In Sec. 4, the intersections of the λ functions of the mass of the droplet for the electrically charged (i.e., EWbgfms) and electrically uncharged (i.e., Wbgfms) configurations are analyzed. Two of such pairs of bgfms configurations are found and analyzed: one with a mass equal to 123.7 GeV and the other with 126.67 GeV. Then, the Wbgfms configuration with a mass equal to 126.67 GeV is interpreted as the state found in the LHC experiment [40,41] (the Wbgfms configuration with a mass equal to 123.7 GeV is also considered). Also, in Sec. 4 the decay and gamma transparency of the Wbgfms configuration are described. After the Conclusions, in Appendix 1 the Table with some quantum numbers of fields in the $SU_L(2) \times U_Y(1)$ CGSW model is given. In Appendix 2, the field equations for the gauge self-fields and the scalar field fluctuation in CGSW model with continuous matter current density fluctuations are given. The calculations below are in the "natural units" $\hbar = c = 1$.

1. BOSON GROUND STATE SOLUTIONS

In the CGSW model the Lagrangian density for the fluctuations and self-fields coupled to them with the hidden $SU_L(2) \times U_Y(1)$ symmetry is as follows:

$$\mathcal{L}_f = -\frac{1}{4}F^a_{\mu\nu}F^{a\mu\nu} - \frac{1}{4}B_{\mu\nu}B^{\mu\nu} + (\nabla_\mu \Phi_f)^+ \nabla^\mu \Phi_f - \\ - \lambda\left(\Phi_f^+\Phi_f - \frac{v^2}{2}\right)^2 + \mathcal{L}_f^f, \quad (1)$$

where $\mathcal{L}_f^{\,f}$ is the fermionic part of the fluctuation sector

$$\mathcal{L}_f^f = i\bar{L}\gamma^\mu\nabla_\mu L_f + i\bar{R}_f\gamma^\mu\nabla_\mu R_f - \sqrt{2}\,\frac{m_f}{v}(\bar{L}_{fL}\Phi_f\, R_f + \text{h.c.}). \quad (2)$$

Here, $v = 246.22$ GeV [42] and $\lambda \neq 0$ is the constant parameter of the scalar fluctuation potential, whose value will be established later on. To simplify the calculations, we neglect the mass m_{ℓ_f} of the fermionic fluctuation.

The fields inside the bgfms droplet are either the classical fluctuations of fields or classical self-fields and in this paper they are treated as such. Because

the formalism for the self-consistent treatment of the quantum fields operators is not known, therefore the fields of the self-consistent approach are not the ones of a quantum field theory origin. The same is true for the quantum fluctuation fields operators. This concerns the scalar fluctuation doublet and all fermionic fluctuations and bosonic self-fields inside the bgfms configuration. Moreover, both the bosonic self-fields and the scalar and fermionic fluctuations that compose the bgfms configuration are not directly observed. What is observed is the droplet of the bgfms configuration. In this respect, the clarifying (only) similarity is to think of the neutron as a kind of configuration of fields. It is hard to prove that it consists of a proton and an electron (although see [43, 44]). Similarly, it would be risky to call the fermionic fluctuation inside the droplet, e.g., a particular lepton fluctuation, although in the CGSW model the field fluctuations inside the droplet are granted the $SU_L(2) \times U_Y(1)$ quantum numbers (see the Table in Appendix 1). For example, the electrically charged EWbgfms state found in Sec. 4 has the $SU_L(2) \times U_Y(1)$ quantum numbers of the fermionic fluctuation(s), which are the same as the numbers of the positron. Also, the scalar fluctuation potential $\lambda(\Phi_f^+\Phi_f - v^2/2)^2$ in the CGSW model is the one for the classical scalar field *fluctuation* Φ_f that exists inside the bgfms configuration only and not for the Higgs field. In conclusion, the CGSW model is one of the fluctuations of basic (scalar or fermionic) fields and the self-fields coupled to them. The scalar or fermionic fluctuations can be the objects different from the ones known from, e.g., the scattering experiments, but the self-fields $W^{\pm}$, Z, and A, although they are also not the quantum fields in the CGSW model, are the classical counterparts of the Standard Model (SM) bosonic fields and can be named after them.

Finally, the question remains as to what is the host object for the droplet of the bgfms configuration? Let us begin with the similarity of an electron in an atom. The self-field concept, as developed by Barut and Kraus, has been successfully used to compute nonrelativistic and relativistic Lamb shifts [19, 20]. In their approach, the host object is the electron, and the tiny Lamb shift of its wave mechanical energy state arises from the electron fluctuation coupled self-consistently to its classical electromagnetic self-field. The self-consistent solution for the Lamb shift is then obtained iteratively, that is why it is sometimes seen as inferior to the perturbative quantum electrodynamics (QED). In this paper, the situation is similar, but the energy of the host fermion (or fermions), if it was, e.g., the electron (or electronic fluctuation), appears to be minute in comparison to the obtained mass of the bgfms configuration.

In Eqs. (1) and (2), the covariant differentiations ∇_μ for the scalar fluctuation doublet Φ_f and for a fermionic field fluctuations doublet L_f and singlet R_f are

$$\nabla_\mu \Phi_f = \partial_\mu \Phi_f + igW_\mu \Phi_f + \frac{1}{2} ig' Y B_\mu \Phi_f, \tag{3}$$

$$\begin{aligned}\nabla_\mu L_f &= \partial_\mu L_f + igW_\mu L_f + \frac{1}{2}ig'YB_\mu L_f,\\ \nabla_\mu R_f &= \partial_\mu R_f + \frac{1}{2}ig'YB_\mu R_f,\end{aligned} \tag{4}$$

where

$$W_\mu = W_\mu^a \frac{\sigma^a}{2} \tag{5}$$

is the gauge field decomposition with respect to the $su(2)$ algebra generators. The $U_Y(1)$ self-field tensor is defined as

$$B_{\mu\nu} = \partial_\mu B_\nu - \partial_\nu B_\mu, \tag{6}$$

and the $SU_L(2)$ Yang–Mills self-field tensor as

$$F_{\mu\nu}^a = \partial_\mu W_\nu^a - \partial_\nu W_\mu^a - g\varepsilon_{abc}W_\mu^b W_\nu^c, \tag{7}$$

where the symbol ε_{abc} signifies the structure constants for $SU_L(2)$, which are antisymmetric with the interchange of two neighbour indices and $\varepsilon_{123} = +1$.

The fundamental constants of the model are the coupling constant for $SU_L(2)$, which is denoted by g, and the coupling constant for $U_Y(1)$, which according to convention is denoted by $g'/2$. The weak hypercharge operator for the $U_Y(1)$ group is called Y. The quantum numbers in the model are given in the Table (Appendix 1).

Now, the scalar fluctuation doublet

$$\Phi_f = \frac{1}{\sqrt{2}}\begin{pmatrix}0\\ \varphi_f\end{pmatrix} \tag{8}$$

contains the scalar field fluctuation φ_f. We have adopted the notations

$$L_f = \begin{pmatrix}\nu_{fL}\\ \ell_{fL}\end{pmatrix} \quad \text{and} \quad R_f = (\ell_{fR}), \tag{9}$$

where for the sake of transparency only one leptonic fluctuation ℓ inside the bgfms and its neutrino fluctuation are specified. The contribution from other existing fermionic fluctuations can be treated in the similar way.

Now, for our charged (electroweak or weak) physical configuration at $\varphi_f = \delta$, we decompose the *total* self-fields W_μ^a, B_μ and the scalar field fluctuation φ_f, which stay on the LHS of Eq. (10) as follows:

$$\begin{cases} W_\mu^a = \omega_\mu^a + \tilde{W}_\mu^a,\\ B_\mu = b_\mu + \tilde{B}_\mu,\\ \varphi_f = \delta + \tilde{\varphi}_f. \end{cases} \tag{10}$$

Here, each of the total fields on the RHS is decomposed into the *self-consistently* treated parts ω_μ^a, b_μ, and δ and *the wavy* (non-self-consistent) parts $\tilde{W}_\mu^a$, $\tilde{B}_\mu$ of the self-fields and $\tilde{\varphi}_f$ of the scalar field fluctuation, respectively. The wavy terms are not treated self-consistently. In this paper, the thin wall approximation is used in which ω_μ^a, b_μ, and δ are constant. These homogeneous components of the self-fields are the main quantities which we are interested in, and they are searched for self-consistently on the ground state denoted as $(\,)_0$. The other, wavy parts of the self-fields, do not enter into the self-consistent calculation in the presented model. Nevertheless, the wavy parts are important in determining the modified mixing angle Θ (see Eq. (39)) and in estimating the range of the validity of the thin wall approximation.

1.1. The Screening Condition of the Fluctuation of Charges. Now, the effective potential on the ground state is given by

$$\mathcal{U}_f^{\text{eff}} = -\left(\mathcal{L}_f\right)_0, \tag{11}$$

where $\mathcal{L}_f$ is the Lagrangian density (see Eq. (1)) of the CGSW model. Let J_{fY}^μ and $J_f^{a\mu}$ be the continuous matter current density fluctuations extended in space (see Eqs. (80) and (81)) equal on the ground state to

$$J_{fY}^\mu = \left(\overline{L}_f\gamma^\mu Y L_f + \overline{R}_f\gamma^\mu Y R_f\right)_0 \quad \text{and} \quad J_f^{a\mu} = \left(\overline{L}_f\gamma^\mu\frac{\sigma^a}{2}L_f\right)_0, \tag{12}$$

respectively.

We now assume that on the ground state, for the system in the local rest coordinate system we have

$$J_{fY}^0 = \varrho_{fY}, \quad J_{fY}^i = 0, \quad J_f^{a0} = \varrho_f^a, \quad \text{and} \quad J_f^{ai} = 0, \tag{13}$$

where ϱ_{fY} and ϱ_f^a are the matter charge density fluctuations related to $U_Y(1)$ and $SU_L(2)$, respectively. Equation (13) determines the ground state which is not relativistically covariant, hence locally, inside the discussed droplets of the fluctuations, the Lorentz invariance might not be its fundamental property (the symmetry of the Lagrangian density (2) still remaining). Yet, we will see that their diameter in the analyzed cases is only of the order of 0.001 fm (see Subsecs. 2.2 and 3.1).

Remark. This means that although some characteristics of these objects may be detectable, the effects of the violations of the Lorentz invariance might remain undetectable or marginally detectable in the present experiments. Similar to the case of partons, which although small are observed, not all of their characteristics are detectable. The literature on the possibility of the violation of the Lorentz invariance is notable [45–47].

As all of the analyses in this paper that pertain to the ground fields are performed on the ground state, therefore, if it is not necessary, the denotation $(\ )_0$ will be omitted.

Thus, what will finally be found is really the ground state of a system, which follows from the fact that the analyzed droplets of the fields of the excited configurations that lie near the physically interesting solutions have real non-negative squared masses of all their constituent fields. The stability of solutions for the particular configurations of fields is one of the basic problems analyzed in this paper. The particular ground state configurations can decay via radiation or the decay of the constituent fields only. There were attempts to approach to such phenomena on the basis of the self-energy rather than on the basis of the quantized radiation field [48].

The self-fields which are calculated from (11) are the ground state fields and only these self-fields are treated fully self-consistently in this model. The boson fields, W^a_μ, B_μ, and φ_f (see Eq. (10)), which in the ground state of the whole configuration of fields are naturally called the ground fields, are denoted as ω^a_μ, b_μ, and δ, respectively,

$$\text{self-consistent (parts of) self-fields} \quad \begin{cases} W^a_\mu = \omega^a_\mu, \\ B_\mu = b_\mu, \\ \varphi_f = \delta. \end{cases} \tag{14}$$

They are searched for self-consistently.

Next, we assume that also in the decomposition (10) in the excited states of the system, the self-consistent parts ω^a_μ, b_μ of the self-fields and δ are found from the self-consistent analysis of potential $\mathcal{U}^{\text{eff}}_f$ given by Eq. (11) and that in the excited states matter current density fluctuations are the same as J^μ_{fY} and $J^{a\mu}_f$ given by Eqs. (12) and (13).

The self-consistent parts (both on the ground state and on the excited ones) can be parameterized in the following way [2]:

$$\omega^a_\mu = \begin{cases} \omega^a_0 = \sigma\, n^a, \\ \omega^a_i = \vartheta\, \varepsilon_{aib}\, n^b, \quad \text{and} \quad n^a n^a = 1, \end{cases} \tag{15}$$

$$b_\mu = \begin{cases} b_0 = \beta, \\ b_i = 0. \end{cases} \tag{16}$$

In Eq. (15), the $(n^a) = \text{const}$ plays the role of a unit vector in the adjoint representation of the Lie algebra $su(2)$. It determines the direction of the ground fields (or more generally of the self-consistent part of the self-fields). It can be seen that (no summation over index "a")

$$\omega^a_\mu \omega^{a\mu} = \sigma^2 n^a n^a - \vartheta^2 \varepsilon_{aib} \varepsilon_{aib} n^b n^b \quad \text{and} \quad b_\mu b^\mu = \beta^2. \tag{17}$$

Now, further calculations are performed in the thin wall approximation in which ω_μ^a, b_μ, and δ are the homogeneous fields.

Using Eqs. (14)–(16) in Eqs. (11) and (1), we obtain the effective potential

$$\mathcal{U}_f^{\text{eff}}(\vartheta,\sigma,\beta,\delta) = -g^2\sigma^2\vartheta^2 + \frac{1}{2}g^2\vartheta^4 - \frac{1}{8}g^2\delta^2(\sigma^2-2\vartheta^2) + \frac{1}{4}gg'\delta^2\beta\sigma n^3 - \\ - \frac{1}{8}g'^2\delta^2\beta^2 + g\varrho_f^a n^a\sigma + \frac{g'}{2}\varrho_{fY}\beta + \frac{1}{4}\lambda(\delta^2-v^2)^2 \quad (18)$$

for the self-consistent parts of the *self-fields*. For the self-fields on the ground state, the potential $\mathcal{U}_f^{\text{eff}}(\vartheta,\sigma,\beta,\delta)$ forms the complete effective potential.

When the self-consistent parts of fields are homogeneous in time and space, then ϑ, σ, β, and δ are constant, and from $\partial_\nu\vartheta = \partial_\nu\sigma = \partial_\nu\beta = \partial_\nu\delta = 0$, $\nu = 0,1,2,3$, it follows that $\nabla^2\vartheta = \nabla^2\sigma = \nabla^2\beta = \nabla^2\delta = 0$. This means that (in the thin wall approximation) the self-consistent part of the self-fields and the scalar field fluctuation form an incompressible matter. Then, the field equations Eqs. (77)–(79) and Eq. (82) (see Appendix 2) that resulted from the CGSW Lagrangian (1) give the following four algebraic equations for the self-consistent parts ϑ, σ, β of the self-fields and δ of the scalar field fluctuation:

$$\left[\frac{1}{2}\delta^2 - 2\sigma^2 + 2\vartheta^2\right]\vartheta = 0, \quad (19)$$

$$-g\left(2\vartheta^2 + \frac{1}{4}\delta^2\right)\sigma + \frac{1}{4}g'\delta^2\beta n^3 + \varrho_f^a n^a = 0, \quad (20)$$

$$\frac{1}{2}(g\sigma n^3 - g'\beta)\delta^2 + \varrho_{fY} = 0, \quad (21)$$

$$\left[-\frac{1}{4}g^2(\sigma^2-2\vartheta^2) + \frac{1}{2}gg'\sigma\beta n^3 - \frac{1}{4}g'^2\beta^2 + \lambda(\delta^2-v^2)\right]\delta = 0. \quad (22)$$

In the self-consistent homogeneous case, Eqs. (77)–(79) and Eq. (82) are equivalent to

$$\partial_\vartheta\mathcal{U}_f^{\text{eff}} = \partial_\sigma\mathcal{U}_f^{\text{eff}} = \partial_\beta\mathcal{U}_f^{\text{eff}} = \partial_\delta\mathcal{U}_f^{\text{eff}} = 0, \quad (23)$$

and thus Eqs. (19)–(22) can be easily checked. They form the self-consistent part of the *screening condition of the fluctuation of charges*, which is the analog of the screening current condition in electromagnetism [49]. They are used in the calculations of the value of change of the observed electric and weak density fluctuations of charges (see Eqs. (29)–(31) below) and the effective masses of the fields (see Eqs. (33)–(36) below). The self-fields obtained self-consistently, i.e., according to Eqs. (19)–(22), will be called the *self-consistent fields*. The configuration of the self-consistent fields *on the ground state* is called (in agreement with Introduction) the (boson) *ground fields induced by matter sources* (bgfms)

configuration [2]. They can be equivalently obtained self-consistently from the effective potential given by Eqs. (18) and (23).

When we define the "electroweak magnetic field" as $\mathcal{B}_i^a = 1/2\varepsilon_{ijk}F_{jk}^a$ and the "electroweak electric field" as $\mathcal{E}_i^a = F_{i0}^a$, then their self-consistent parts ($\sigma = \text{const}$, $\vartheta = \text{const}$, $\beta = \text{const}$, $(n^a) = \text{const}$) for $\vartheta \neq 0$ are equal to $(\mathcal{B}_i^a)_0$ and $(\mathcal{E}_i^a)_0$, respectively, [2]

$$(\mathcal{B}_i^a)_0 = -g\vartheta^2 n^i n^a \quad \text{and} \quad (\mathcal{E}_i^a)_0 = g\sigma\vartheta(\delta_{ai} - n^a n^i). \tag{24}$$

Now, let us choose

$$(n^a) = (0, 0, 1). \tag{25}$$

In this case, the self-consistent parts of the electroweak magnetic field $(\mathcal{B}_3^3)_0 = -g\vartheta^2$ along the x^3 spatial direction and of the electroweak electric field $(\mathcal{E}_1^1)_0 = (\mathcal{E}_2^2)_0 = g\sigma\vartheta$ pointing in the x^1 and x^2 spatial directions, respectively, are different from zero.

Let us perform (for $\delta \neq 0$) a "rotation" of W_μ^3 and B_μ self-fields to the physical self-fields Z_μ and A_μ

$$\begin{pmatrix} Z_\mu \\ A_\mu \end{pmatrix} = \begin{pmatrix} \cos\Theta & -\sin\Theta \\ \sin\Theta & \cos\Theta \end{pmatrix} \begin{pmatrix} W_\mu^3 \\ B_\mu \end{pmatrix}. \tag{26}$$

Then, consequently a rotation of σ and β self-consistent fields to their counterparts ζ and α (and similarly for $\tilde{Z}_\mu$ and $\tilde{A}_\mu$), as well as a rotation of the charge density fluctuations ϱ_f^3 and ϱ_{fY} to their corresponding physical quantities ϱ_{fZ} and ϱ_{fQ}, are as follows:

$$\begin{pmatrix} \zeta \\ \alpha \end{pmatrix} = \begin{pmatrix} \cos\Theta & -\sin\Theta \\ \sin\Theta & \cos\Theta \end{pmatrix} \begin{pmatrix} \sigma \\ \beta \end{pmatrix}, \tag{27}$$

$$\begin{pmatrix} (g/\cos\Theta)\varrho_{fZ} \\ (g\sin\Theta)\varrho_{fQ} \end{pmatrix} = \begin{pmatrix} \cos\Theta & -\sin\Theta \\ \sin\Theta & \cos\Theta \end{pmatrix} \begin{pmatrix} (g)\varrho_f^a n^a \\ (g'/2)\varrho_{fY} \end{pmatrix}. \tag{28}$$

It is worthwhile to write the relations between weak isotopic charge density fluctuation ϱ_f^3 (see Eqs. (13) and (25)), weak hypercharge density fluctuation ϱ_{fY}, standard relation (SR) unscreened electric charge density fluctuation $\varrho_{fQ\,\mathrm{SR}}$ (Eq. (31) below), standard (SR) unscreened weak charge density fluctuation $\varrho_{fZ\,\mathrm{SR}}$ (Eq. (31) below) and their generalizations in our model, i.e., the observed electric charge density fluctuation ϱ_{fQ} and the observed weak charge density fluctuation ϱ_{fZ}:

$$\varrho_{fQ} = \varrho_{fQ\,\mathrm{SR}} + \frac{1}{2}\left(\frac{g'}{g}\operatorname{cotan}\Theta - 1\right)\varrho_{fY}, \tag{29}$$

$$\varrho_{fZ} = \varrho_f^3 - \varrho_{fQ}\sin^2\Theta, \tag{30}$$

$$\varrho_{fQ\,\mathrm{SR}} = \varrho_f^3 + \frac{1}{2}\varrho_{fY}, \quad \text{and} \quad \varrho_{fZ\,\mathrm{SR}} = \varrho_f^3 - \varrho_{Q\,\mathrm{SR}}\sin^2\Theta_W. \tag{31}$$

Here, Θ is the modified mixing angle (given below), whereas the Standard Model (SM) relations between the Weinberg angle Θ_W, g, and g' are given by $\cos\Theta_W = \dfrac{g}{\sqrt{g^2+g'^2}}$ and $\sin\Theta_W = \dfrac{g'}{\sqrt{g^2+g'^2}}$.

The numerical calculations are performed with the Fermi coupling constant equal to $G_F \approx 1.16638\cdot 10^{-5}$ GeV^{-2}, the SM value for the boson $W^{\pm}$ mass, $m_{W\,\mathrm{SM}} \approx 80.385$ GeV, and $\sin^2\Theta_W \approx 0.23116$ [42]. From these values, $g = \sqrt{8m_{W\,\mathrm{SM}}^2 G_F/\sqrt{2}} \approx 0.65295$, $g' = g\tan\Theta_W \approx 0.35803$, and $v = 2m_{W\,\mathrm{SM}}/g \approx 246.22$ GeV are calculated. The accuracy of the results is restricted by the accuracy of the measurement of the boson $W^{\pm}$ mass (80.385 ± 0.015) GeV [42], i.e., to the fourth significant digits.

1.2. The Masses of the Self-Fields and Scalar Field Fluctuation. The massive Lagrangian density for the boson self-fields and the scalar field fluctuation, which follows from the kinematical part of the Lagrangian (1), is equal to

$$\begin{aligned}\mathcal{L}_{\mathrm{mass}} = &-\frac{1}{2}g^2\varepsilon_{abc}\varepsilon_{ade}\omega_\mu^b\omega^{d\mu}\tilde{W}_\nu^c\tilde{W}^{e\nu} + \frac{1}{8}g^2\delta^2\tilde{W}_\mu^a\tilde{W}^{a\mu} - \\ &- \frac{1}{4}gg'\delta^2\tilde{W}_\mu^3\tilde{B}^\mu + \frac{1}{8}g'^2\delta^2\tilde{B}_\mu\tilde{B}^\mu + \frac{1}{8}g^2\omega_\mu^a\omega^{a\mu}\tilde{\varphi}_f^2 - \\ &- \frac{1}{4}gg'\omega_\mu^3 b^\mu\tilde{\varphi}_f^2 + \frac{1}{8}g'^2 b_\mu b^\mu\tilde{\varphi}_f^2 - \frac{1}{2}\lambda(3\delta^2 - v^2)\tilde{\varphi}_f^2. \quad (32)\end{aligned}$$

This changes the effective potential (11) for the excited states by $\tilde{\mathcal{U}}_f^{\mathrm{eff}} = -\mathcal{L}_{\mathrm{mass}}$.

Using Eqs. (14)–(17) and Eq. (25) in the massive Lagrangian density (32), we obtain the following squared masses [2] for (the wavy parts of) the boson self-fields and the scalar field fluctuation (10) inside a droplet of the bgfms configuration:

$$m_{\tilde{W}^{1,2}}^2 = g^2\left(\frac{1}{4}\delta^2 - \sigma^2 + \vartheta^2\right), \quad (33)$$

$$m_{\tilde{W}^3}^2 = g^2\left(\frac{1}{4}\delta^2 + 2\vartheta^2\right), \quad (34)$$

$$m_{\tilde{B}}^2 = \frac{1}{4}g'^2\delta^2, \quad (35)$$

$$m_{\tilde{\varphi}_f}^2 = \lambda(3\delta^2 - v^2) - \frac{1}{4}g^2(\sigma^2 - 2\vartheta^2) + \frac{1}{2}gg'\sigma\beta n^3 - \frac{1}{4}g'^2\beta^2. \quad (36)$$

Let us note that the masses in Eqs. (33)–(36) are modified (near the ground state of the droplet) according to the self-consistent part of the screening current condition given by Eqs. (19)–(22).

After using Eq. (26), we pass from the fields $\tilde{B}$ and $\tilde{W}^3$ to their physical linear combinations $\tilde{A}$ and $\tilde{Z}$, and from (32) we obtain their squared masses

$$m^2_{\tilde{Z}} = \frac{1}{2}\left[m^2_{Z\,\mathrm{SR}} + 2g^2\vartheta^2 + \sqrt{(m^2_{Z\,\mathrm{SR}} + 2g^2\vartheta^2)^2 - 2(gg'\delta\vartheta)^2}\right], \tag{37}$$

$$m^2_{\tilde{A}} = \frac{1}{2}\left[m^2_{Z\,\mathrm{SR}} + 2g^2\vartheta^2 - \sqrt{(m^2_{Z\,\mathrm{SR}} + 2g^2\vartheta^2)^2 - 2(gg'\delta\vartheta)^2}\right], \tag{38}$$

where from the orthogonality property of the mass matrix of the fields $\tilde{A}$ and $\tilde{Z}$ the modified mixing angle Θ is obtained:

$$\tan\Theta = \frac{-(1+8(\vartheta/\delta)^2)g^2 + g'^2}{2gg'} + \sqrt{\left(\frac{(1+8(\vartheta/\delta)^2)g^2 - g'^2}{2gg'}\right)^2 + 1}. \tag{39}$$

In Eqs. (37)–(38), $m^2_{Z\,\mathrm{SR}}$ looks similar to the standard relation (SR) for the boson Z^μ squared mass

$$m^2_{Z\,\mathrm{SR}} \equiv \frac{1}{4}(g^2 + g'^2)\,\delta^2. \tag{40}$$

Defining the complex self-fields $W^\pm_\mu = (W^1_\mu \mp iW^2_\mu)/\sqrt{2}$ from Eq. (32), the squared masses also follow (compare with Eq. (33)):

$$m^2_{\tilde{W}^\pm} = g^2\left[\frac{1}{4}\delta^2 - (\zeta\,\cos\Theta + \alpha\,\sin\Theta)^2 + \vartheta^2\right]. \tag{41}$$

Finally, the squared mass of the scalar field fluctuation is equal to

$$m^2_{\tilde{\varphi}_f} = \lambda(3\delta^2 - v^2) - \frac{1}{\delta^2}(m^2_{\tilde{Z}}\zeta^2 - m^2_{\tilde{A}}\alpha^2) + \\ + 2g^2\left(\frac{1}{\delta^2}(\zeta\,\cos\Theta + \alpha\,\sin\Theta)^2 + \frac{1}{4}\right)\vartheta^2. \tag{42}$$

From Eqs. (19)–(22) and (27), we notice that with the simultaneous change of the signs of ϱ^3_f and ϱ_{fY}, the signs of β, σ, α, and ζ also change but such physical characteristics as the modified mixing angle Θ given by Eq. (39) and the above masses of the fields inside the bgfms configuration and the mass of the droplet of the bgfms configuration, calculated (further on) using the potential Eq. (18), remain invariant.

The calculations below are carried out in the stationary points given by Eq. (23) of the effective potential $\mathcal{U}^{\mathrm{eff}}_f$ of the self-consistent fields. It is not difficult to see that the solutions of Eqs. (19)–(22) for the ground fields in these points of the effective potential $\mathcal{U}^{\mathrm{eff}}_f$ split into the two cases discussed below, one for the EWbgfms configuration and the other for the Wbgfms one.

It is evident from Eq. (39) that the transition from the zero charge density fluctuations to $\varrho_f^3 \neq 0$, $\varrho_{fY} \neq 0$ is associated with the nonlinear response of the system. It can also be noticed that electroweak SM assumptions, which concern the relations between charges, are formally recovered for $\vartheta = 0$. Some quantum numbers of the CGSW $SU_L(2) \times U_Y(1)$ model are given in the Table in Appendix 1.

2. THE EWbgfms FIELDS CONFIGURATIONS WITH $\varrho_{fQ\,\mathrm{SR}} \neq 0$

Now, Eqs. (19)–(22) can be rewritten as follows:

$$\sigma = \frac{1}{2g\vartheta^2}\varrho_{fQ\,\mathrm{SR}}, \tag{43}$$

$$\beta = \frac{1}{g'}\left(g\sigma n^3 + 2\frac{\varrho_{fY}}{\delta^2}\right), \tag{44}$$

$$\vartheta^6 + \frac{1}{4}\delta^2\vartheta^4 - \frac{1}{4g^2}\varrho_{fQ\,\mathrm{SR}}^2 = 0, \tag{45}$$

$$\delta^6 + \left(\frac{g^2}{2\lambda}\vartheta^2 - v^2\right)\delta^4 - \frac{1}{\lambda}\varrho_{fY}^2 = 0. \tag{46}$$

Note. From Eq. (45), we see that the self-consistent field ϑ is nonzero only if $\varrho_{fQ\,\mathrm{SR}} \neq 0$. We also see that according to Eq. (46) (compare with Eq. (21)), the nonzero value of ϱ_{fY} implies the nonzero self-consistent field $\delta \neq 0$ of the scalar fluctuation φ_f.

Now Eqs. (14)–(16) with (27) read

$$\begin{cases} W_{0,3}^{\pm} = 0, \quad W_1^{\pm} = \pm i\vartheta/\sqrt{2}, \quad W_2^{\pm} = \vartheta/\sqrt{2}, \\ Z_i = 0, \quad Z_0 = \zeta, \quad \text{where} \quad (\zeta = \sigma\,\cos\,\Theta - \beta\,\sin\,\Theta), \\ A_i = 0, \quad A_0 = \alpha, \quad \text{where} \quad (\alpha = \sigma\,\sin\,\Theta + \beta\,\cos\,\Theta), \\ \varphi_f = \delta. \end{cases} \tag{47}$$

Let us note that the relation between the weak hypercharge quantum number Y and the electric charge quantum number Q can be written in the form $Q = pY/2$ (for matter fields), where the corresponding values of $p\,(p \neq 0)$ are given in the Table in Appendix 1. Then the relation between the weak hypercharge density fluctuation ϱ_{fY} and the standard electric charge density fluctuation $\varrho_{fQ\,\mathrm{SR}}$ can also be written in the form

$$\varrho_{fQ\,\mathrm{SR}} = p\frac{\varrho_{fY}}{2}, \tag{48}$$

where different values of p (see the Table) represent different matter fields which can be the sources of charge density fluctuations.

The above-mentioned screening charge phenomenon now quantified by Eqs. (43)–(46) is of crucial importance for the characteristics of the bgfms configurations analyzed below. When the scalar fluctuation field φ_f together with $W^{\pm}_{1,2}$, Z_0, A_0-gauge self-fields with the nonzero self-consistent parts given by Eq. (47) are present, then the electroweak magnetic and electric ground fields (24) penetrate inside the whole spatially extended fermionic fluctuation. In their presence, the electroweak force generates an "electroweak screening fluctuation of charges" in accord with Eqs. (43)–(46) and Eqs. (29)–(31). This is connected with the fact that the basic fermionic field fluctuation carries a nonzero charge.

2.1. Characteristics of the EWbgfms Configuration. The solutions of Eqs. (43)–(46) with the condition (48) were previously discussed in [2]. The numerical results of this analysis for the self-consistent parts of fields, the scalar fluctuation δ and self-fields β, σ, ϑ, and for the physical self-fields α and ζ (see Eq. (27)) as functions of the electric charge density fluctuation ϱ_{fQ} for $p = 2$ are presented in Fig. 1, *a*. One particular value of $\lambda \approx 0.0652$ has been chosen, the choice of which will be argued later on. The plots for different values of λ and p can be found in [1]. Here, we notice only that the physical charge density fluctuation ϱ_{fQ} (see Eq. (29)) for the EWbgfms configuration for different values of p (see the Table) converge for relatively small values of ϱ_{fQ}, i.e., for values of the charge density fluctuation ϱ_{fQ} in the range of up to values approximately 10^3 times bigger than those that correspond to the matter densities in the nucleon. Also, the ratio $\varrho_{fQ}/\varrho_{fQ\,\mathrm{SR}} \to 1$ for $\varrho_{fQ\,\mathrm{SR}} \to 0$ (see Fig. 2, *a*). As a result, all of the physical characteristics of the bgfms configurations for different values of p (see the Table) converge with $\varrho_{fQ} \to 0$ [1]. This can be noticed, e.g.,

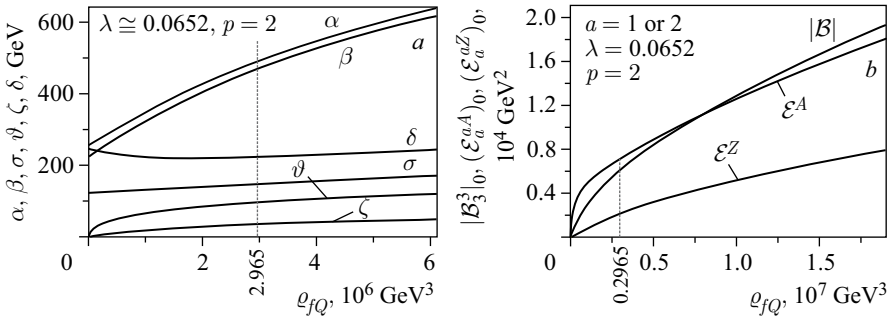

Fig. 1. *a*) The self-consistent parts α, β, σ, ϑ, ζ of the self-fields A_0, B_0, $W^{a=3}_{i=0}$, $W^{a=1}_{i=2}$–$W^{a=2}_{i=1}$, and Z_0, respectively, as functions of the electric charge density fluctuation $\varrho_{fQ}(\vartheta \neq 0, \delta \neq 0)$, Eq. (29). The self-consistent field δ of the self-field φ_f as the function of $\varrho_{fQ}(\vartheta \neq 0, \delta \neq 0)$. *b*) The self-consistent parts $(\mathcal{E}^{aA}_a)_0 = g \sin\Theta\,\alpha\,\vartheta$, $(\mathcal{E}^A)$, of the "electromagnetic electric ground fields" and $(\mathcal{E}^{aZ}_a)_0 = g \cos\Theta\,\zeta\,\vartheta$, $(\mathcal{E}^Z)$, $a = 1, 2$, of the "weak electric ground fields" (see Eqs. (24), (25) and (27)) and $|(\mathcal{B}^3_3)_0| = |-g\vartheta^2|$, $(|\mathcal{B}|)$, of the absolute value of "electroweak magnetic ground field" as functions of ϱ_{fQ}

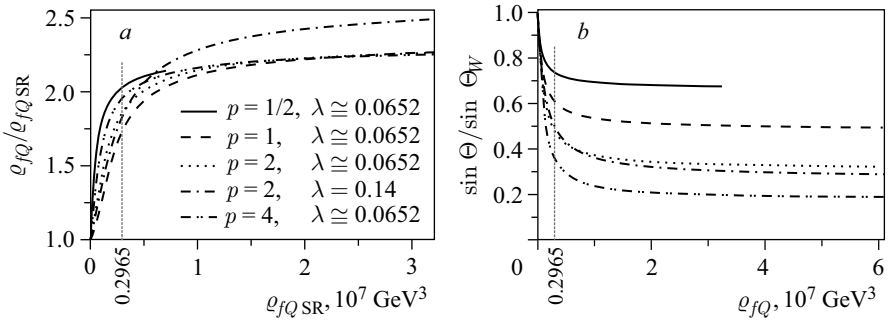

Fig. 2. *a*) The ratio of the observed electric charge density fluctuation ϱ_{fQ} (see Eq. (44)) to the standard electric charge density fluctuation $\varrho_{fQ\,\mathrm{SR}}$ ($\vartheta \neq 0$, $\delta \neq 0$) as the function of $\varrho_{fQ\,\mathrm{SR}}(\vartheta \neq 0,\ \delta \neq 0)$. *b*) The ratio $\sin\Theta/\sin\Theta_W$ (see Eq. (39)) as the function of $\varrho_{fQ}(\vartheta \neq 0,\ \delta \neq 0)$

from the behavior of the ratio $\sin\Theta/\sin\Theta_W$ (Fig. 2, *b*) as a function of ϱ_{fQ}, where Θ is the modified mixing angle given by Eq. (39). On the other hand, $\varrho_{fQ}/\varrho_{fQ\,\mathrm{SR}} \to C = \mathrm{const} > 1$ for $\varrho_{fQ\,\mathrm{SR}} \to \infty$, where the value of C depends both on p and λ (see Fig. 2, *a*). It can be noticed that the dependence of C on the parameter λ of the scalar fluctuation potential is stronger than on p. In principle, for bigger values of $\varrho_{fQ\,\mathrm{SR}}$ the information on the true value of λ should be extracted from the slope C of the asymptote to the plot of ϱ_{fQ} as the function of $\varrho_{fQ\,\mathrm{SR}}$.

From Eqs. (19) and (33) (for $\vartheta \neq 0$), it can be noticed that fields $\tilde{W}^+$ and $\tilde{W}^-$ (see Eq. (47)), taken together as a pair of massive fields, become *inside* the EW-bgfms configuration the *massless* self-fields that are coupled to the charge density fluctuations $\varrho_{fQ} \neq 0$ ($\varrho_{fQ\,\mathrm{SR}} \neq 0$ and $\varrho_{fY} \neq 0$). The results for the dependence of the masses of $\tilde{A}$, $\tilde{Z}$, and $\tilde{\varphi}_f$ fields (see Eqs. (38), (37), and (42)) inside the EWbgfms configuration on the electric charge density fluctuation $\varrho_{fQ}(\vartheta \neq 0,\ \delta \neq 0)$ are presented in Fig. 3, *a*.

Let us notice that the expressions (37) for $m^2_{\tilde{Z}}$ and (38) for $m^2_{\tilde{A}}$ have a root. For a particular value of $p < 1.388 \approx 2\sqrt{\sin\Theta_W}$ and below some value of $\lambda = \lambda_Z$ (which depends on p), the expression $(m^2_{Z\,\mathrm{SR}} + 2g^2\vartheta^2)^2 - 2(gg'\delta\vartheta)^2$ under this root gets above some value of ϱ_{fQ} the negative sign, so that the EWbgfms configuration becomes unstable in the $\tilde{Z}$ and $\tilde{A}$ field sectors. Thus, for $p < 1.388$ and a particular value $\lambda < \lambda_Z$, there is a value of ϱ_{fQ} for which $m_{\tilde{A}} = m_{\tilde{Z}}$.

For example, for $p = 1/2$ the limiting value $\lambda_Z \approx 0.2148$. Thus, e.g., for $\lambda = 0.14 < \lambda_Z$ this expression becomes negative above $\varrho_{fQ} \approx 1.767 \cdot 10^8\ \mathrm{GeV}^3$ (for which $\mathcal{E}_{\mathrm{st}}(\varrho_{fQ}) \approx 8.313 \cdot 10^{10}\ \mathrm{GeV}^4$). For $p = 1/2$ and $\lambda = 0.0652 < \lambda_Z$,

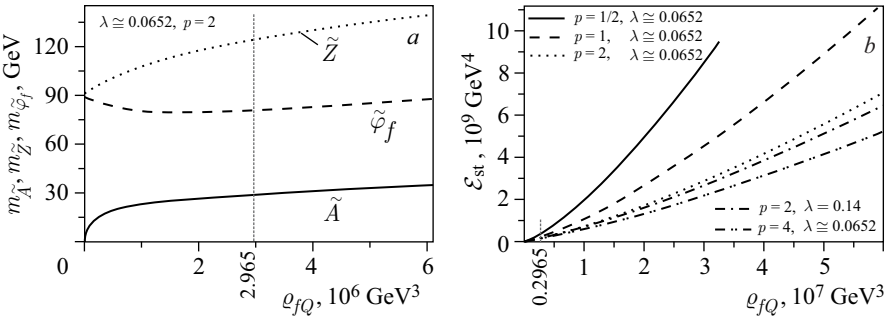

Fig. 3. *a*) The masses $m_{\tilde{A}}$, $m_{\tilde{Z}}$, and $m_{\tilde{\varphi}_f}$ of the gauge boson fields $\tilde{A}^\mu$ and $\tilde{Z}^\mu$ and of the scalar field fluctuation $\tilde{\varphi}_f$, respectively, as functions of the electric charge density fluctuation ϱ_{fQ} ($\vartheta \neq 0$, $\delta \neq 0$). *b*) The energy density $\mathcal{E}_{\rm st}(\varrho_{fQ})$, (49), of the EWbgfms configuration for boson ground fields calculated self-consistently according to Eqs. (43)–(46) (for all values of $p \neq 0$ from the Table) as the function of ϱ_{fQ}

this expression becomes negative above $\varrho_{fQ} \approx 1.531 \cdot 10^7$ GeV^3 (for which $\mathcal{E}_{\rm st}(\varrho_{fQ}) \approx 3.456 \cdot 10^9$ GeV^4). Next, e.g., for $p = 1$ the limiting value $\lambda_Z \approx 0.0297$. It will be shown in Sec. 4 that the value of ϱ_{fQ} for a physically interesting EWbgfms configuration (e.g., the state $s2$ in Sec. 4) (for which this instability might potentially appear) is smaller than the mentioned limiting value of ϱ_{fQ}. Moreover, above $p \approx 1.388$ and thus also from $p = 3/2$ upwards, the discussed configurations do not possess this instability in the $\tilde{Z}$ and $\tilde{A}$ field sectors for all values of λ and ϱ_{fQ}.

2.2. The Mass of the EWbgfms Configuration. The energy density given by Eq. (18) for stationary (st) solutions of the EWbgfms configuration for boson ground fields, calculated self-consistently according to Eqs. (43)–(46) as the function of ϱ_{fQ}, is equal to

$$\mathcal{E}_{\rm st}(\varrho_{fQ}) = \mathcal{U}_f^{\rm eff}(\vartheta \neq 0, \delta \neq 0) \quad \text{(with fields treated self-consistently).} \tag{49}$$

The energy density $\mathcal{E}_{\rm st}(\varrho_{fQ})$ increases both with ϱ_{fQ} and $\varrho_{fQ\,\rm SR}$. The plots of the dependence of $\mathcal{E}_{\rm st}(\varrho_{fQ})$ for boson ground fields given by Eqs. (43)–(46) on the electric charge density fluctuation ϱ_{fQ} are presented in Fig. 3, *b* (for values of $p \neq 0$ from the Table). We notice that from the point of view of $\mathcal{E}_{\rm st}(\varrho_{fQ})$, the EWbgfms configurations fall into classes of p that differ weakly with λ inside a particular class (which is shown in Fig. 3, *b* for $p = 2$ only).

The matter electric charge fluctuation of an electrically charged EWbgfms configuration is equal to

$$q_f = \frac{4}{3}\pi r_{q_f}^3\, \varrho_{fQ}, \tag{50}$$

where r_{q_f} is the "radius of the charge density fluctuation" in the thin wall approximation. The radius r_{q_f} is the function of ϱ_{fQ}. The mass of the electrically charged EWbgfms configuration is equal to

$$M_{q_f} = \frac{4}{3}\pi r_{q_f}^3 \mathcal{E}_{\rm st}(\varrho_{fQ}) \quad \text{and} \quad M_{q_f} = \pm q_f M_{q_f=1}, \tag{51}$$

where, because of the Pauli exclusion principle used for the fermionic fluctuations, we obtain that $q_f = \pm 1$ or ± 2 only inside one droplet (except the cases that the consecutive fermionic fluctuations occupy their higher energy states). When the fermionic fluctuation (one or two in each bgfms configuration of fields) that plays the role of the matter source that induces boson ground fields was taken into account in the calculation of mass M_{q_f}, then its value would be changed by an order of the energy of this fermionic fluctuation. In this paper, the energy of the fermionic fluctuation is neglected.

The functional dependence of the mass M_{q_f} of a droplet of the EWbgfms configuration of fields (with charge fluctuation q_f) on $r_{q_f}(\varrho_{fQ})$ is presented in Fig. 4, *a*. It exhibits a minimum in r_{q_f} (and also in ϱ_{fQ}) for some values of p. For instance (see [1]), for $p = 2$ and with $\lambda \approx 0.0652$, it has the minimal value $M_{q_f} = \pm q_f \cdot 63.335$ GeV at $\varrho_{fQ} = 2.965 \cdot 10^6$ GeV^3 ($\varrho_{fQ\,\rm SR} = 1.788 \cdot 10^6$ GeV^3)

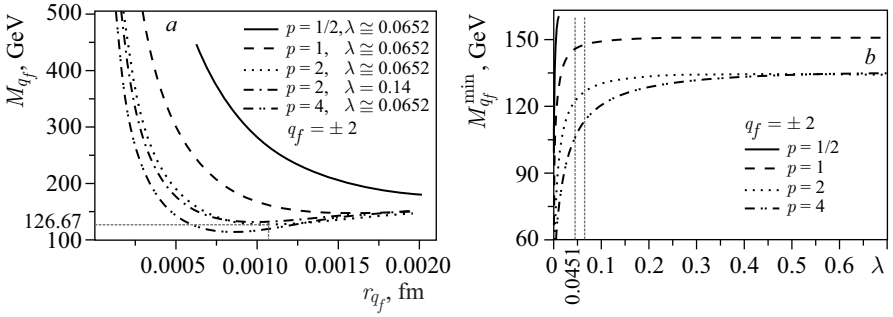

Fig. 4. *a*) The mass $M_{q_f=\pm 2}$ of the EWbgfms configuration as a function of the radius r_{q_f} (for $p \neq 0$ from the Table and exemplary λ's). The curves with $p \geqslant 1$ exhibit local minima. For example, the minimal $M_{q_f=\pm 2}$ for $p = 2$ and $\lambda \approx 0.0652$ is equal to $M^{\rm min}_{q_f=\pm 2} = 126.67$ GeV for $r_{q_f} \approx 0.00107$ fm. The figures are plotted up to the values of r_{q_f} smaller than $1/m_{\tilde{Z}}$ (see Fig. 3, *a*). For $p = 1/2$ values of ϱ_{fQ} are no bigger than $3.297 \cdot 10^7$ GeV^3 (for which $r_{q_f=2} \approx 0.000481$ fm), as above it the configuration becomes unstable ($m^2_{\tilde{Z}}$ (37) and $m^2_{\tilde{A}}$ (38) become imaginary). For $p = 1/2$ and for $\lambda > 0.0119$, there are no EWbgfms configurations with local minimum of $M_{q_f}(r_{q_f})$. *b*) The minimal mass $M^{\rm min}_{q_f}$ of the EWbgfms configuration as a function of λ. In the case of $p = 1/2$, the thin wall approximation is not fulfilled and there are also no EWbgfms configurations with local minimum of $M_{q_f}(r_{q_f})$ for $\lambda > 0.0119$; hence, we see the cut in the curve above this value (compare with the text under Fig. 4, *a*)

and $\mathcal{E}_{\rm st}(\varrho_{fQ}) = 1.878 \cdot 10^8$ GeV^4 with the radius of the corresponding charge density fluctuation $r_{q_f} = q_f^{1/3} \cdot 0.000852$ fm. In comparison, for a proton with a global electric charge $Q = 1$, its electric charge radius $r_Q \approx 0.805$ fm.

Finally, let us suppose that in the process a droplet of the EWbgfms configuration with a particular $p \geqslant 1$ appears. This self-consistent charged EWbgfms configuration lies in the *minimum* of the function of mass $M_{q_f=2}$ vs. ϱ_{fQ} (or r_{q_f}) (see Fig. 4, *a*). Its self-consistent (homogeneous) self-fields are the solution of the equations of motion (77)–(79) and (82). If necessary, we will mark this *minimal mass* by $M_{q_f}^{\rm min}$. This stationary state is the resonance via the weak interactions only and can disintegrate through simultaneous decay or radiation of its constituent fields. The most interesting fact is that the closest configuration of fields is an electrically neutral Wbgfms configuration with the same mass. Because their masses are equal, hence their Breit–Weisskopf–Wigner probability density has a dispersion of the same order.

Note. From Fig. 3, *b* we see that $\mathcal{E}_{\rm st} \to 0$ as $\varrho_{fQ\,\rm SR} \to 0$ ($\varrho_{fQ} \to 0$) for all of the values of $\lambda > 0$ and $p \neq 0$ considered (see the Table). For $\varrho_{fQ} \to 0$ and for all of the considered values of $\lambda > 0$ and $p \neq 0$ (see the Table) from Eq. (18) and Eqs. (43)–(46), we also obtain

$$M_{q_f} \to \pm q_f g v/2 = \pm q_f \cdot 80.385 \text{ GeV}, \tag{52}$$

where the sign "+" is for $q_f > 0$ and sign "−" is for $q_f < 0$. Yet, as in this limit the EWbgfms configuration inside a droplet does not reproduce the uncharged SM configuration (for which $\varrho_{fQ} = 0$), thus even for $q_f = \pm 1$ this bgfms configuration cannot be interpreted as the observed, well-known $W^{\pm}$ boson particle.

Indeed, even if the charge density fluctuation tends in the limit to zero $\varrho_{fQ} \to 0$ and thus we obtain $\vartheta \to 0$ and $\zeta \to 0$ for the ground fields of the $W^+ - W^-$ pair and Z, respectively, yet, the result is that the self-consistent ground field α of A_0 is still nonzero in this limit (see Eq. (47) and Fig. 1, *a*) [1]. Therefore, the transition from the configuration of fields with $\varrho_{fQ} \neq 0$ ($\varrho_{fQ\,\rm SR} \neq 0$ and $\varrho_{fY} \neq 0$) to the configuration with $\varrho_{fQ} = 0$ (then with $\varrho_{f\,\rm SR} = 0$, $\varrho_{fY} = 0$, $\alpha = 0$, $\zeta = 0$, and $\vartheta = 0$) inside the droplet of the EWbgfms configuration is not a continuous one. Let us notice that in the double limit $\varrho_{fQ} \to 0$ and $q_f \to 0$, we obtain $M_{q_f} = 0$.

3. Wbgfms CONFIGURATIONS WITH $\varrho_{fZ\,\rm SR} \neq 0$

From Eq. (39), it can be noticed that for $\vartheta = 0$ the standard relation $\tan\Theta = \tan\Theta_W = g'/g$ is held; hence, from Eqs. (29)–(31) it follows that $\varrho_{fZ} = \varrho_{fZ\,\rm SR}$ and $\varrho_{fQ} = \varrho_{fQ\,\rm SR}$. The other possibility $\tan\Theta = -g/g' = -\operatorname{cotan}\Theta_W$ obtained in this case from Eq. (39) is not a physical solution.

Using Eqs. (27)–(28), we can rewrite the effective potential $\mathcal{U}_f^{\text{eff}}$ given by Eq. (18) for the ground fields in the following form:

$$\mathcal{U}_f^{\text{eff}}(\zeta,\alpha,\delta) = \sqrt{g^2+g'^2}\,\varrho_{fZ\,\text{SR}}\,\zeta + \frac{g\,g'}{\sqrt{g^2+g'^2}}\,\varrho_{fQ\,\text{SR}}\,\alpha - \\ - \frac{1}{8}(g^2+g'^2)\,\delta^2\zeta^2 + \frac{1}{4}\lambda\,(\delta^2-v^2)^2. \quad (53)$$

For $\vartheta = 0$, we can rewrite Eqs. (20)–(22) as follows:

$$\varrho_{fQ\,\text{SR}} = 0, \quad (54)$$

$$\frac{1}{4}\sqrt{g^2+g'^2}\,\delta^2\,\zeta = \varrho_{fZ\,\text{SR}} \quad (55)$$

and

$$\lambda\,(\delta^2-v^2) - \frac{1}{4}(g^2+g'^2)\,\zeta^2 = 0. \quad (56)$$

The relations (54)–(56) form the self-consistent part of the screening condition of the fluctuation of charges.

Note. Thus, according to Eq. (55), the nonzero weak charge density fluctuation $\varrho_{fZ\,\text{SR}}$ inevitably leads to the nonzero self-consistent field ζ of Z_μ. The nonzero $\varrho_{fZ\,\text{SR}}$ also implies the nonzero self-consistent field $\delta \neq 0$ of the scalar fluctuation φ_f (compare with the Note below Eq. (46)).

Using Eq. (53) and equations (compare with Eq. (23))

$$\partial_\alpha \mathcal{U}_f^{\text{eff}} = 0, \quad (57)$$

and

$$\partial_\zeta \mathcal{U}_f^{\text{eff}} = \partial_\delta \mathcal{U}_f^{\text{eff}} = 0, \quad (58)$$

the relations (54)–(56) can be easily checked.

Two nontrivial relations given by Eqs. (55)–(56) lead to the solution

$$\delta^2(\varrho_{fZ\,\text{SR}}) = \frac{4\,\varrho_{fZ\,\text{SR}}}{\sqrt{g^2+g'^2}\zeta}, \quad (59)$$

and

$$\zeta(\varrho_{fZ\,\text{SR}}) = \frac{2}{3^{1/2}\,(g^2+g'^2)^{1/2}} \times \\ \times \frac{\lambda^{-1/3}\left(3^{3/2}\,\varrho_{fZ\,\text{SR}} + \sqrt{27\,\varrho_{fZ\,\text{SR}}{}^2 + \lambda\,v^6}\right)^{2/3} - v^2}{\lambda^{-2/3}\left(3^{3/2}\,\varrho_{fZ\,\text{SR}} + \sqrt{27\varrho_{fZ\,\text{SR}}{}^2 + \lambda\,v^6}\right)^{1/3}}, \quad (60)$$

where self-consistent fields ζ and δ are the functions of $\varrho_{fZ\,\text{SR}}$ only (see Fig. 5, *a*). Using Eqs. (15)–(16) and (26)–(27), we can rewrite Eq. (14) for the self-consistent field α of A_μ in the form

$$A_\mu = (\alpha, 0, 0, 0). \quad (61)$$

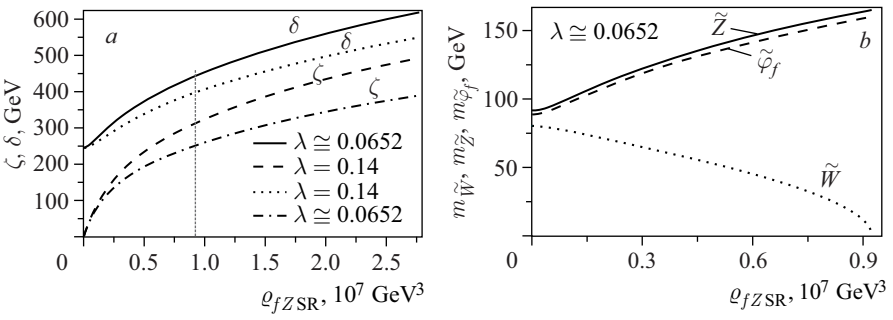

Fig. 5. *a*) The self-consistent fields ζ of Z_0 and δ of φ_f as the function of the (standard) weak charge density fluctuation $\varrho_{fZ\,\mathrm{SR}}$ ($\vartheta = 0$, $\delta \neq 0$, $\varrho_{fQ\,\mathrm{SR}} = 0$). In the limit $\varrho_{fZ\,\mathrm{SR}} \to 0$, the self-consistent ground fields tend to the uncharged values $\zeta = 0$ and $\delta = v$. *b*) The masses $m_{\tilde{W}^\pm}$ (Eq. (67)), $m_{\tilde{Z}}$ (Eq. (65)) of the wavy part of $W_\mu^\pm$ and Z_μ, respectively, and the mass $m_{\tilde{\varphi}_f}$ (Eq. (68)) of the wavy part of φ_f inside the droplet of the Wbgfms configuration as the function of $\varrho_{fZ\,\mathrm{SR}}$ ($\vartheta = 0$, $\delta \neq 0$, $\varrho_{fQ\,\mathrm{SR}} = 0$). In the limit $\varrho_{fZ\,\mathrm{SR}} \to 0$, these masses tend to the uncharged (i.e., for $\varrho_{fZ\,\mathrm{SR}} = 0$) values $m_{W^\pm} = gv/2$, $m_Z = \sqrt{g^2 + g'^2}\,v/2$, and $m_{\varphi_f} = \sqrt{2\lambda}\,v$, respectively

From Eqs. (54)–(56) and (60)–(69) below, it follows that α is not a dynamical variable. It corresponds to a nonphysical degree of freedom and can be removed by the gauge transformation $\alpha \to 0$. Thus, $U_Q(1)$ remains the valid symmetry group giving (see Eq. (27))

$$\alpha = \sigma \sin \Theta_W + \beta \cos \Theta_W = 0. \tag{62}$$

Now, the self-consistent fields (14) can be rewritten as follows:

$$\begin{cases} W_\mu^{1,2} = 0, \quad W_i^3 = 0, \\ W_0^3 = -\beta \operatorname{cotan} \Theta_W, \\ B_0 = \beta, \\ B_i = 0, \\ \varphi_f = \delta, \end{cases} \tag{63}$$

or in terms of physical fields

$$\begin{cases} W_\mu^\pm = 0, \quad Z_i = 0, \\ Z_0 = \zeta, \quad \text{where} \quad \zeta = -\dfrac{1}{\sin \Theta_W}\beta, \\ A_\mu = 0, \\ \varphi_f = \delta. \end{cases} \tag{64}$$

The appearance of the nonzero weak charge density fluctuation $\varrho_{fZ\,\mathrm{SR}}$ and the self-consistent field ζ of the self-field Z_μ induced by it (see Eq. (60)) influences

the masses of the wavy parts of the boson self-fields and of the scalar field fluctuation. Their squares inside a droplet of the Wbgfms configuration are, according to Eqs. (37)–(38), (41)–(42) (for $\vartheta = 0$), equal to (see Fig. 5, *b*)

$$m^2_{\tilde{Z}} = \frac{1}{4}(g^2 + g'^2)\delta^2, \tag{65}$$

$$m^2_{\tilde{A}} = 0, \tag{66}$$

$$m^2_{\tilde{W}^\pm} = \frac{1}{4}g^2(\delta^2 - 4\zeta^2\,\cos^2\,\Theta_W), \tag{67}$$

$$m^2_{\tilde{\varphi}_f} = \lambda\,(3\delta^2 - v^2) - \frac{1}{4}(g^2 + g'^2)\,\zeta^2. \tag{68}$$

Thus, the effective mass of the wavy part of the physical self-field A_μ is equal to $m_{\tilde{A}} = 0$.

After putting the self-consistent ground fields calculated according to Eqs. (55), (56) together with Eq. (54) into Eq. (53), the energy density for the stationary solution of the Wbgfms configuration, $\mathcal{E}_{\rm st}(\delta, \varrho_{fZ\,\rm SR}) = \mathcal{U}_f^{\rm eff}$ $(\delta, \varrho_{fZ\,\rm SR};\ \vartheta = 0,$ $\varrho_{fQ\,\rm SR} = 0)$ is obtained [1]

$$\mathcal{E}_{\rm st}(\delta, \varrho_{fZ\,\rm SR}) = 2\frac{\varrho^2_{fZ\,\rm SR}}{\delta^2} + \frac{1}{4}\,\lambda\,(\delta^2 - v^2)^2 \tag{69}$$

(with δ treated self-consistently), which after using Eqs. (55) and (56) could also be rewritten as follows (see Fig. 6):

$$\mathcal{E}_{\rm st}(\varrho_{fZ\,\rm SR}) = \frac{1}{2}\sqrt{g^2 + g'^2}\zeta(\varrho_{fZ\,\rm SR})\times \\ \times\left(\varrho_{fZ\,\rm SR} + \frac{1}{32\lambda}(g^2 + g'^2)^{3/2}\zeta^3(\varrho_{fZ\,\rm SR})\right), \tag{70}$$

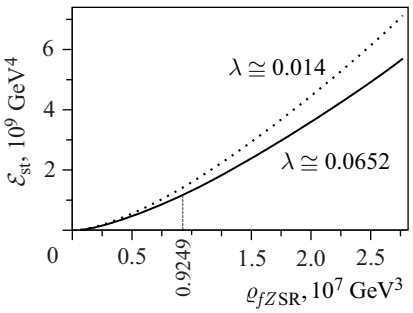

Fig. 6. The energy density of the Wbgfms configuration $\mathcal{E}_{\rm st}(\varrho_{fZ\,\rm SR}) = \mathcal{U}_f^{\rm eff}$ $(\vartheta = 0,$ $\delta \neq 0,\ \varrho_{fQ\,\rm SR} = 0)$ (see Eq. (70))

where the self-consistent ground field $\zeta = \zeta(\varrho_{fZ\,\mathrm{SR}})$ is the function of $\varrho_{fZ\,\mathrm{SR}}$ (see Eq. (60)).

From Eqs. (67) and (59), it is clear that the appearance of $\varrho_{fZ\,\mathrm{SR}} > 0$ (so $\zeta > 0$) leads to the instability in the $W^{\pm}_{\mu}$ sector only if

$$\zeta^3(\varrho_{fZ\,\mathrm{SR}}) > \frac{\sqrt{g^2 + g'^2}\,\varrho_{fZ\,\mathrm{SR}}}{g^2}, \tag{71}$$

which is connected with the fact that then $m^2_{\tilde{W}^{\pm}} < 0$ [1]. When the equality $\zeta^3(\varrho_{fZ\,\mathrm{SR}}) = \sqrt{g^2 + g'^2}\,\varrho_{fZ\,\mathrm{SR}}/g^2$ is taken into account, we obtain the relationship between $\lambda_{\max}$ and $\varrho_{fZ\,\mathrm{SR\,max}}$, where $\lambda_{\max}$ is the value of λ and $\varrho_{fZ\,\mathrm{SR\,max}}$ is the value of $\varrho_{fZ\,\mathrm{SR}}$ for which we have $m^2_{\tilde{W}^{\pm}} = 0$. The region of stable Wbgfms configurations with $\zeta \neq 0$ is on and below the $\varrho_{fZ\,\mathrm{SR\,max}}(\lambda_{\max})$ boundary curve (see Fig. 7, *a*).

For the weak charge density fluctuation $\varrho_{fZ\,\mathrm{SR}} < \varrho^{\mathrm{limit}}_{fZ\,\mathrm{SR}} \equiv (g^2 + g'^2) \times v^3/(8g) \approx 1.585 \cdot 10^6$ GeV^3, this configuration of fields is stable for an arbitrary λ (see Fig. 7, *a*). For values of $\varrho_{fZ\,\mathrm{SR}}$ bigger than $\varrho^{\mathrm{limit}}_{fZ\,\mathrm{SR}}$, the Wbgfms configuration

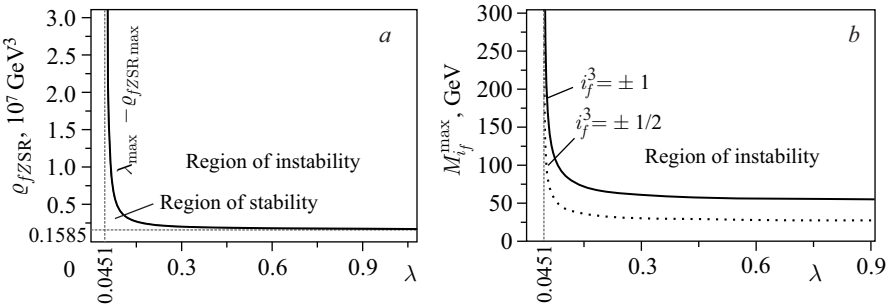

Fig. 7. *a*) The partition of the $(\lambda, \varrho_{fZ\,\mathrm{SR}})$ plane into the regions of stability and instability of the Wbgfms configurations with $\varrho_{fZ\,\mathrm{SR}} \neq 0$. The region of stable Wbgfms configurations lies on and below $\varrho_{fZ\,\mathrm{SR\,max}}(\lambda_{\max})$ boundary curve, where $\lambda_{\max}$ is the value of λ and $\varrho_{fZ\,\mathrm{SR\,max}}$ is the value of $\varrho_{fZ\,\mathrm{SR}}$ for which $m^2_{W^{\pm}} = 0$. The limiting values $\varrho^{\mathrm{limit}}_{fZ\,\mathrm{SR}} \approx 0.1585 \cdot 10^7$ GeV^3 and $\lambda_{\mathrm{limit}} \approx 0.0451$ are shown. *b*) The upper mass $M^{\max}_{i^3_f}$ (according to the stability of the Wbgfms configuration in the $W^{\pm}$ sector) with $\varrho_{fZ\,\mathrm{SR}} \neq 0$ as a function of $\lambda = \lambda_{\max}$, where $m^2_{\tilde{W}^{\pm}} = 0$ for points $(\lambda_{\max},\ M^{\max}_{i^3_f})$ which lie on the curve. The region of possible Wbgfms configurations is on and below the $M^{\max}_{i^3_f}(\lambda_{\max})$ boundary curve. Two such curves, the first one for $i^3_f = \pm 1$ and the second one for $i^3_f = \pm 1/2$ are plotted. For $\lambda \to \infty$, $M^{\max}_{i^3_f = \pm 1} \approx 52.277$ GeV and $M^{\max}_{i^3_f = \pm 1/2} \approx 26.138$ GeV, respectively

is unstable for a given λ above a certain value of $\varrho_{fZ\,\mathrm{SR}}$, which is equal to

$$\varrho_{fZ\,\mathrm{SR\ max}} = \frac{8g^2\lambda^{3/2}\,(g^2+g'^2)\,v^3}{[16g^2\lambda-(g^2+g'^2)^2]^{3/2}}. \tag{72}$$

For $\lambda < \lambda_{\mathrm{limit}} \equiv (g^2+g'^2)^2/(16g^2) \approx 0.0451$, the Wbgfms configuration is stable for all values of $\varrho_{fZ\,\mathrm{SR}}$ (see Fig. 7, *a*).

3.1. The Mass of the Wbgfms Configuration. Let us examine the mass of the droplet of the Wbgfms configuration induced by the nonzero weak charge density fluctuation $\varrho_{fZ\,\mathrm{SR}}$:

$$M_{i_f^3} = \frac{4}{3}\pi r_{i_f^3}^3\,\mathcal{E}_{\mathrm{st}}(\varrho_{fZ\,\mathrm{SR}}) \quad \text{and} \quad M_{i_f^3} = \pm i_f^3 M_{i_f^3=1}, \tag{73}$$

where $\mathcal{E}_{\mathrm{st}}(\varrho_{fZ\,\mathrm{SR}})$ is given by Eq. (70) and the sign "+" is for $i_f^3 > 0$ and "−" is for $i_f^3 < 0$. Because of the Pauli exclusion principle used for the fermionic fluctuations, only $i_f^3 = \pm 1/2$ or ± 1 (see the Table) inside one droplet are possible (except in cases where the consecutive fermionic fluctuations occupy their higher energy states). Here, $r_{i_f^3}$ is the "radius of the weak charge density fluctuation" determined by the weak isotopic charge fluctuation inside the Wbgfms configuration in the thin wall approximation

$$i_f^3 = \frac{4}{3}\pi r_{i_f^3}^3\,\varrho_{fZ\,\mathrm{SR}}. \tag{74}$$

The radius $r_{i_f^3}$ is the function of i_f^3. The value of $|i_f^3|$ inside one droplet can possibly be more than 1 for the composite fermion fluctuation only [50].

According to the stability of the Wbgfms configuration in respect of the $W^{\pm}$ sector, we can also obtain the upper limit $M_{i_f^3}^{\max}$ for the value of the mass $M_{i_f^3}$. The region of the stability of possible Wbgfms configurations lies on and below the proper $M_{i_f^3}^{\max}(\lambda_{\max})$ boundary curve (see Fig. 7, *b*). Two such curves are presented, one for the function $M_{i_f^3=\pm 1}^{\max}(\lambda)$ and the other for $M_{i_f^3=\pm 1/2}^{\max}(\lambda)$. In principle, the value of λ can be readout from the particular curve when the experimental value of the mass $M_{i_f^3}^{\max}$ is known.

Note. It is not difficult to see that $\varrho_{fZ\,\mathrm{SR}} \to 0$ (which implies $\zeta \to 0$ and $\delta \to v$) entails $\mathcal{E}_{\mathrm{st}}(\varrho_{fZ\,\mathrm{SR}}) \to 0$ for the energy density (70) of the limiting Wbgfms configuration. The double limit $\varrho_{fZ\,\mathrm{SR}} \to 0$ and $i_f^3 \to 0$ is the only possibility for obtaining the weakly uncharged Wbgfms configuration. From Fig. 7, *b* it can be noticed that for the established value of $\lambda > \lambda_{\mathrm{limit}} \approx 0.0451$ and with $i_f^3 \to 0$, the maximal mass $M_{i_f^3}$ of the Wbgfms configuration, which lies on the boundary curve $M_{i_f^3}^{\max}(\lambda_{\max})$, also tends to zero. Thus, in this case

in the double limit $\varrho_{fZ\,\mathrm{SR}} \to 0$ and $i_f^3 \to 0$, the Wbgfms configuration becomes necessarily massless for $\lambda > \lambda_{\mathrm{limit}}$ (for $\lambda \leqslant \lambda_{\mathrm{limit}}$ this would be not necessarily the case).

At the same time, from Fig. 5, *a*, *b* we notice that for $\varrho_{fZ\,\mathrm{SR}} \to 0$, the Wbgfms configuration reproduces some characteristics of the uncharged $\varrho_{fZ\,\mathrm{SR}} = 0$ configuration, e.g., the masses of the (composite) boson fields and the lack of self-consistent gauge fields. Nevertheless, even for an infinitesimally small value of $\varrho_{fZ\,\mathrm{SR}}$, the value of the self-consistent field δ is different from zero and tends in the limit to v. Thus, for $\lambda > \lambda_{\mathrm{limit}}$ (which will be suggested later on) and for $\varrho_{fZ\,\mathrm{SR}} \to 0$, $i_f^3 \to 0$, the particles interacting with this massless Wbgfms configuration can perceive the fields that are inside a Wbgfms droplet with their SM values of couplings.

4. THE INTERSECTIONS OF EWbgfms AND Wbgfms CONFIGURATIONS

Let us start with the electrically charged EWbgfms configuration with a matter electric charge fluctuation equal to $q_f = 2$ (analysis for $q_f = -2$ would be the same) and a minimal mass $M^{\min}_{q_f=2}$. Now, let us pose the question on the configuration of the nearest Wbgfms droplet with $\varrho_{fZ\,\mathrm{SR}} \neq 0$ that arises after the decay of this minimal mass EWbgfms configuration with $\varrho_{fQ} \neq 0$. The solution with a particular value of λ can be found as the point of the intersection of the function of the minimal masses $M^{\min}_{q_f}(\lambda)$ of EWbgfms configurations (presented in Fig. 4, *b*) with the function of the maximal masses $M^{\max}_{i_f^3}(\lambda)$ of Wbgfms configurations (presented in Fig. 7, *b*). Six such solutions can be seen in Fig. 8, *a*.

The estimates obtained for the mass of the observed neutral state in the LHC experiment [51–53] are in case of the CMS detector equal currently to $(126.2 \pm 0.6\,(\mathrm{stat.}) \pm 0.2\,(\mathrm{syst.}))$ GeV for its $ZZ^{(*)} \to 4\ell$ ($\ell = e$ or μ) decay channel [40] and in case of the ATLAS detector equal to $(126.6 \pm 0.3\,(\mathrm{stat.}) \pm 0.7\,(\mathrm{syst.}))$ GeV in the $\gamma\gamma$ channel or $(123.5 \pm 0.8\,(\mathrm{stat.}) \pm 0.3\,(\mathrm{syst.}))$ GeV in the $ZZ^{(*)} \to 4\ell$ channel [41]. Therefore, from the estimates obtained in the LHC experiment, only two solutions for the intersection of functions $M^{\max}_{i_f^3}(\lambda)$ (one for $i_f^3 = \pm 1/2$ and the other for ± 1) with the function of the minimal masses $M^{\min}_{q_f=2}(\lambda)$ for $p = 2$ remain. These are the solutions $s1$ and $s2$, which are discussed below.

For the solution $s1$ in Fig. 8, *a*, we obtain $\lambda \approx 0.065187 \approx 0.0652$ and $M^{\min}_{q_f=\pm 2} = M^{\max}_{i_f^3=\pm 1} \approx 126.67$ GeV. Firstly, let us write down the characteristics of the electrically charged EWbgfms configuration with $\varrho_{fQ} \neq 0$ (see Eq. (47) and Fig. 1, *a*). Thus, the electric charge density fluctuation is equal to $\varrho_{fQ} = 2.965 \cdot 10^6$ GeV^3 (compare with Fig. 2, *a*), and the energy density (Fig. 3, *b*) is equal to $\mathcal{E}_{\mathrm{st}}(\varrho_{fQ}) \approx 1.878 \cdot 10^8$ GeV^4. For $q_f = 2$ the radius of the electrically

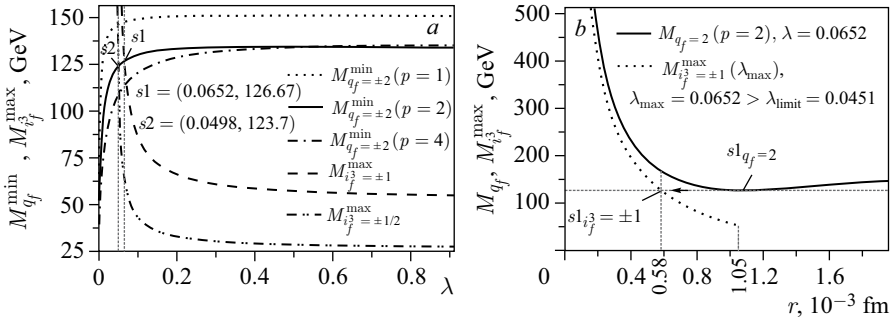

Fig. 8. *a*) The intersections of the curves of the minimal masses $M^{\min}_{q_f}(\lambda)$ of the EWbgfms configurations (presented in Fig. 4, *b*) with the curves of the maximal masses $M^{\max}_{i^3_f}(\lambda)$ of the Wbgfms configurations (presented in Fig. 7, *b*). *b*) The EWbgfms configurations with the mass $M_{q_f=2}$ as a function of the radius $r_{q_f=2}$ and the Wbgfms configurations with the upper mass $M^{\max}_{i^3_f=\pm1}(r_{i^3_f})$ (according to the stability in the $W^{\pm}$ sector) as a function of the radius $r_{i^3_f=\pm1}$. The "decomposition" of the particular solution $s1$ found in Fig. 8, *a* is shown. Two points, i.e., $s1_{q_f=2}$ with $M^{\min}_{q_f=2}(r_{q_f}) \approx 126.67$ GeV on the curve $M_{q_f=2}(r_{q_f})$ and $s1_{i^3_f=\pm1}$ with the same mass on the curve $M^{\max}_{i^3_f=\pm1}(r_{i^3_f})$ correspond to one point $s1$ in Fig. 8, *a*. The right cut $r^{\text{int}}_{q_f=2} \sim 1/m_Z \approx 0.00196$ fm on the curve $M_{q_f=2}(r_{q_f})$ is connected with the thin wall approximation, whereas for the curve $M^{\max}_{i^3_f=\pm1}(r_{i^3_f})$ the maximal value of $r_{i^3_f=\pm1} \approx 0.00105$ fm follows from the fact that for $\lambda \to \infty$ the limiting, lowest possible value of $\varrho_{fZ\,\text{SR}}$ for these upper mass configurations is equal to $\varrho^{\text{limit}}_{fZ\,\text{SR}} \approx 1.585 \cdot 10^6$ GeV^3 (see Fig. 7, *a*)

charged EWbgfms configuration is equal to $r_{q_f} \approx 0.00107$ fm (see Figs. 4, *a* and 8, *b*). For $\varrho_{fQ} = 2.965 \cdot 10^6$ GeV^3, the mass $m_{\tilde{Z}} \approx 124.128$ GeV inside the droplet of the EWbgfms configuration is the biggest one (see Fig. 3, *a*); hence, the interaction range $r^{\text{int}}_{q_f}$ inside the droplet is of the order $r^{\text{int}}_{q_f} \sim 1/m_{\tilde{Z}} \approx 0.00159$ fm, and because the ratio $r_{q_f}/r^{\text{int}}_{q_f} \approx 0.675 < 1$, it is reasonable to use the thin wall approximation.

The other, i.e., the electrically neutral Wbgfms configuration of the solution $s1$ with the nonzero weak charge density fluctuation $\varrho_{fZ\,\text{SR max}} \approx 9.249 \cdot 10^6$ GeV^3, has the energy density $\mathcal{E}_{\text{st}}(\varrho_{fZ\,\text{SR max}}) \approx 1.172 \cdot 10^9$ GeV^4 (Fig. 6). For $i^3_f = \pm1$ its radius is equal to $r_{i^3_f} \approx 0.000583$ fm (see Fig. 8, *b*). For this value of $\varrho_{fZ\,\text{SR max}}$, the mass $m_{\tilde{Z}} = 165.064$ GeV (see Fig. 5, *b*) is the biggest one ($m_{\tilde{\varphi}_f} = 160.071$ GeV); hence, the interaction range $r^{\text{int}}_{i^3_f}$ inside the droplet of the Wbgfms configuration is of the order $r^{\text{int}}_{i^3_f} \sim 1/m_{\tilde{Z}} \approx 0.0012$ fm. Thus, because the ratio $r_{i^3_f=1}/r^{\text{int}}_{i^3_f} \approx 0.488 < 1$, it is reasonable to use the thin wall approximation.

The transition from the electrically charged EWbgfms configuration (state $s1_{q_f=2}$) to the uncharged Wbgfms configuration (state $s1_{i_f^3=\mp 1}$) is presented in Fig. 8, *b*. These two points are represented by one solution $s1$ on the $\lambda - M$ plane in Fig. 8, *a*. We interpret the electrically uncharged Wbgfms configuration represented by the point $s1_{i_f^3=\mp 1}$ as the candidate for the neutral state of the mass ~ 126.5 GeV recently observed in the LHC experiment.

Remark. In this paper, the masses of the states $s1_{q_f=+2}$ and $s1_{i_f^3}$ (or $s2_{q_f=+2}$ and $s2_{i_f^3}$) are equal. Yet, the mass splitting between the states $s1_{q_f=+2}$ and $s1_{i_f^3}$ (or $s2_{q_f=+2}$ and $s2_{i_f^3}$) could be of the 10 MeV order, which is in agreement with the value of the decay width of the 126.5 GeV boson state observed in the LHC experiment [54, 55] (also Subsec. 4.1). Then, examples a11–b2 given below, which have on their right-hand sides the dielectron events plus neutrinos, are from this point of view not excluded by the present LHC experiment.

The examples of the processes connected with $s1$ are as follows.

For $s1_{q_f=+2}$ and $s1_{i_f^3=\pm 1}$, which are the leptonic states:

a11) $p+p \to (s1_{q_f=+2}) + X + 2\nu$ and then $(s1_{q_f=+2}) \to (s1_{i_f^3=-1}) + 2\nu + 2e^+$,

a12) $p+p \to (s1_{q_f=+2}) + X + 2\nu$ and then $(s1_{q_f=+2}) \to (s1_{i_f^3=+1}) + 2\bar{\nu} + 2e^+$.

For $s1_{q_f=+2}$ and $s1_{i_f^3=\pm 1}$, which are the baryonic states:

a2) $p+p \to (s1_{q_f=+2}) + X + \binom{\nu\ell^+}{\bar{\nu}\ell^-}$ and then $(s1_{q_f=+2}) \to (s1_{i_f^3=\mp 1}) + 2\nu + 2e^+$.

Here ℓ is the electron or muon and X signifies some jets.

For the solution $s2$ in Fig. 8, *a*, we obtain, correspondingly, $\lambda \approx 0.04977 \approx 0.0498$ and $M^{\min}_{q_f=\pm 2} = M^{\max}_{i_f^3=\pm 1/2} \approx 123.7$ GeV. The characteristics of the electrically charged EWbgfms configuration are as follows: $\varrho_{fQ} \approx 2.615 \cdot 10^6$ GeV^3, $\mathcal{E}_{\rm st}(\varrho_{fQ}) \approx 1.618 \cdot 10^8$ GeV^4, and for $q_f = 2$ the radius of the droplet is equal to $r_{q_f} \approx 0.00112$ fm. For this value of ϱ_{fQ} the mass $m_{\tilde{Z}} \approx 121.940$ GeV is the biggest one; hence, the interaction range $r^{\rm int}_{q_f}$ inside the droplet of the EWbgfms configuration is of the order $r^{\rm int}_{q_f} \sim 1/m_{\tilde{Z}} \approx 0.00162$ fm. Because $r_{q_f}/r^{\rm int}_{q_f} \approx 0.692 < 1$, it is reasonable to use the thin wall approximation. The characteristics of the electrically neutral Wbgfms configuration are as follows: $\varrho_{fZ\,{\rm SR\,max}} \approx 5.477 \cdot 10^7$ GeV^3 with $\mathcal{E}_{\rm st}(\varrho_{fZ\,{\rm SR\,max}}) \approx 1.355 \cdot 10^{10}$ GeV^4, and for $i_f^3 = \pm 1/2$ we obtain $r_{i_f^3} \approx 0.000256$ fm. For this value of $\varrho_{fZ\,{\rm SR\,max}}$, the mass $m_{\tilde{Z}} = 298.621$ GeV is the biggest one ($m_{\tilde{\varphi}_f} \approx 253.036$ GeV); hence, $r^{\rm int}_{i_f^3} \sim 1/m_{\tilde{Z}} \approx 0.000661$ fm. Because $r_{i_f^3}/r^{\rm int}_{i_f^3} \approx 0.387 < 1$, it is reasonable to use the thin wall approximation. The exemplary processes for the $s2$ case (see Fig. 8, *a*) are as follows.

For $s2_{q_f=+2}$ and $s2_{i_f^3=\pm 1/2}$, which are the leptonic states:

b11) $p+p \to (s2_{q_f=+2}) + X + 2\nu$ and then $(s2_{q_f=+2}) \to (s2_{i_f^3=-1/2}) + \nu + 2e^+$,

b12) $p+p \to (s2_{q_f=+2}) + X + 2\nu$ and then $(s2_{q_f=+2}) \to (s2_{i_f^3=+1/2}) + \bar{\nu} + 2e^+$.

For $s2_{q_f=+2}$ and $s2_{i_f^3=\pm 1/2}$, which are the baryonic states:

b2) $p+p \to (s2_{q_f=+2})+X+\binom{\nu\ell^+}{\bar{\nu}\ell^-}$ and then $(s2_{q_f=+2}) \to (s2_{i_f^3=\mp 1/2})+2\nu+2e^+$.

Some of the above-mentioned processes look like the lepton number violation (i.e., a12, b11, and b12), but if s_{q_f} and $s_{i_f^3}$ are leptonic states, they are not really of this type.

If the LHC state can be either a baryonic or leptonic one, then the $q_f = 2$ possibility is chosen only on the basis of the observed mass. Next, if the droplets of the bgfms configurations are leptonic, then the states with $|q_f| > 2$ are (by the Pauli exclusion principle) possible only if the consecutive fermionic fluctuations are in higher energy states. Nevertheless, in both cases, the baryonic and leptonic, the particular function $M_{q_f}^{\min}(\lambda)$ for the EWbgfms configurations with $|q_f| > 2$ intersects with the functions $M_{i_f^3}^{\max}(\lambda)$ of the Wbgfms configurations for higher masses, and these solutions have not yet been observed in the LHC experiment.

Let us consider the case when the bgfms configurations s_{q_f} and $s_{i_f^3}$ are occupied by two (electrically charged and uncharged, respectively) fermionic fluctuations with opposite spin projections. In addition to the scalar fluctuation φ_f, there are four gauge self-fields inside the configuration given by Eq. (47) and three inside the configuration given by Eq. (64). Thus, for the particular configuration of the ground fields given by Eq. (47), its EWbgfms s_{q_f} droplet can have spin zero (and zero to four for its excitations). Meanwhile, for the particular configuration of the ground fields given by Eq. (64), its Wbgfms $s_{i_f^3}$ droplet can have spin zero (and zero to three for its excitations [56–59]). Indeed, because $s_{i_f^3=\pm 1}$ is the ground state configuration, hence the self-consistent field Z_0 exists only inside its droplet (see Eq. (64)), which belongs to the spin zero subspace of the 3-dimensional rotation group. Thus, the $s_{i_f^3=\pm 1}$ ground configuration of fields, which consists of two opposite spin fermionic fluctuations, the scalar fluctuation $\varphi_f = \delta$ and spin zero $Z_0 = \zeta$, has a spin equal to zero. When boosted the Z self-field is longitudinally polarized, i.e., its spin is equal to one with a spin projection equal to zero. Next, from the point of view of the possible value of the spin of the Wbgfms configuration, considerations similar to the ones above (for two fermionic fluctuations) lead to the conclusion that states $s_{i_f^3=\mp 1/2}$ in b11, b12, and b2 with quantum numbers for fermionic fluctuation like those in the Table *are excluded* by the LHC experiment, as they consist of one fermionic fluctuation only thus having a half spin value.

We see that only cases a11, a12, and a2 are possible, and thus the present day experiments have selected the state $s1_{i_f^3=\mp 1}$ with mass $M_{i_f^3=\mp 1}^{\max} \approx 126.67$ GeV for $\lambda \approx 0.0652$ and rejected the state $s2_{i_f^3=\mp 1/2}$ with mass $M_{i_f^3=\mp 1/2}^{\max} \approx 123.7$ GeV

for $\lambda \approx 0.0498$. However, the basic fields that induce the bgfms configurations of fields are (in this model) the fermionic fluctuations; hence, one could think that the states $s_{q_f=2}$ and $s_{i_f^3=\mp 1}$ are leptonic states (think of some models of a neutron in which the neutron is a composition of a baryonic proton and a fermionic electron [43, 44]). In this case, only the possibility of a leptonic state $s1_{i_f^3=\mp 1}$ remains, which is exemplified by processes a11 and a12. Otherwise, the baryonic states exemplified by processes a2 remain with the configuration $s1_{i_f^3=\mp 1}$ suggested as the solution for the state observed in the LHC experiment.

In Fig. 8, *a*, three pairs of neighbouring solutions can be noticed. Nevertheless, whether besides the experimentally noticeable state $s1_{i_f^3=\pm 1}$, the neighbouring solution $s2_{i_f^3=\mp 1/2}$ together with the remaining ones have been also observed [60–63] as more shallow resonances and not as the statistical flukes in the data only, remains an open question. The reason is that in such a case λ gains two additional indexes, i.e., $\lambda \to \lambda_{p,i_f^3}$, where the *electric charge to hypercharge ratio index* p, Eq. (48), numbers the EWbgfms configurations and the *weak isotopic charge* $i_f^3 = \mp 1/2, \mp 1$ numbers the Wbgfms ones.

Thus, in Fig. 8, *a* for each p, where $p = 1, 2$, and 4, one pair $\begin{pmatrix} s_{i_f^3=\mp 1/2} \\ s_{i_f^3=\mp 1} \end{pmatrix}$ of the neighbouring solutions:

$$\begin{pmatrix} (0.0512, 108.79) \\ (0.0705, 114.91) \end{pmatrix}, \begin{pmatrix} (0.0498, 123.7) \\ (0.0652, 126.67) \end{pmatrix} \text{ and } \begin{pmatrix} (0.0484, 146.33) \\ (0.0593, 147.4) \end{pmatrix}, \qquad (75)$$

respectively, can be noticed, where for each of the six solutions the values of λ and $M_{i_f^3}^{\max}$ [GeV] are given.

The central column in Eq. (75) is $\begin{pmatrix} s2_{i_f^3=\mp 1/2} \\ s1_{i_f^3=\mp 1} \end{pmatrix}$. It is easy to notice that the algebraic mean of the mass of two central neighbouring solutions $s1_{i_f^3=\pm 1}$ and $s2_{i_f^3=\mp 1/2}$ is equal to 125.185 GeV. This value is consistent with the mean mass of the configurations observed in the first run of the LHC experiment (with higher than 5σ significance of the observed excess over the expected background [64]). Yet, it has to be also noticed that the values in the third column in Eq. (75) lie in the vicinity of the events recorded in the CMS experiment at a mass of approximately 145 GeV with a statistical significance of $\sim 3\sigma$ above background expectations [60, 62, 65].

Finally, it is not difficult numerically to check that for all Wbgfms configurations that lie on their boundary curve $M_{i_f^3}^{\max}(\lambda_{\max})$ and have a particular value

of the weak isotopic charge fluctuation i_f^3, the relation

$$\frac{4}{3}\,\pi r_{i_f^3}^3\,\delta^3/(3\pi) \approx |i_f^3| \tag{76}$$

is fulfilled (up to the fourth digit after the decimal point). The mass of the droplet calculated with δ obtained from the perfect equality in Eq. (76) with the (non-self-consistent) use of Eq. (49) agrees with $M_{i_f^3}^{\max}$ up to the seventh digit after the decimal point. Thus, the relation (76) is also fulfilled by the configuration $s1_{i_f^3=\mp 1}$ (and e.g., $s2_{i_f^3=\mp 1/2}$ also). The Wbgfms configuration $s1_{i_f^3=\mp 1}$ is the successor of the EWbgfms configuration $s1_{q_f=2}$. In Fig. 8, *a*, these configurations overlap. Both have a mass equal to 126.67 GeV, which (besides the spin zero) has been interpreted above as the signature of the LHC state. In this way, both the charge $q_f = 2$ and $i_f^3 = \pm 1$ are discreetly chosen. Thus, it is suggested by Eq. (76) that in the one parametric $\varrho_{fZ\,\mathrm{SR}} \neq 0$ case (see Eqs. (59) and (60)), the quantization $i_f^3 = \pm 1$ is the artefact of the self-consistency conditions given by Eqs. (55) and (56). The analysis of condition (76) will be discussed in the following paper.

4.1. The Decay of the $s1_{i_f^3=\mp 1}$ Droplet. In the full self-consistent field theory, fields have the same type of couplings as their counterparts in the perturbative quantum field theory. This is the case of, e.g., the self-consistent electrodynamics and one of its outcomes is the derivation of the Lamb shift by Barut and Kraus [19]. Although the presented CGSW model treats the self-consistent field and the wave self-field of excited states differently, a self-field is in reality one object (on the ground state, i.e., in the droplet of a bgfms configuration, only self-consistent fields are present). Thus, both the self-consistent field and the wave self-field in CGSW have the same type of couplings as their counterparts in the GSW model.

The self-consistent electrically uncharged Wbgfms configuration $s1_{i_f^3=\mp 1}$ is the resonance via the weak interactions only and can disintegrate through the simultaneous decay or radiation of its constituents. In a droplet of a Wbgfms configuration of fields induced by $\varrho_{fZ\,\mathrm{SR}} \neq 0$ (with $\varrho_{fQ\,\mathrm{SR}} = 0$), the self-consistent fields φ_f and Z (see Eq. (64)) are present in addition to the background fermionic fluctuations. Then, only δ of φ_f and the time component ζ of Z are different from zero. Due to $\varrho_{fQ\,\mathrm{SR}} = 0$ and $m_A = 0$, the electromagnetic self-field A is totally absent even in the excitation; however, the pair W^+–W^- of the self-fields can appear in the excitation. The self-consistent fields are the initial ones that take part in the decay of the Wbgfms configuration. For each initial self-consistent field the calculation of the coherent transition probability is performed separately (i.e., for $\varphi_f = \delta$ and Z_0), and then the decay of the droplet of the Wbgfms configurations is calculated in accordance with the following scenario. Firstly, there appears the decay of the coupling of the self-consistent

field ζ of Z_μ to the basic fermionic field followed by the decay of ζ (which is very rapid in SM). Then, (for $\varrho_{fZ\,\mathrm{SR}} \to 0$, $i_f^3 \to 0$, and $\lambda > \lambda_{\mathrm{limit}}$) the fields configuration of the droplet decays (see Note in Subsec. 3.1). In this limit, the particles interacting with the configuration can perceive, with the SM values of couplings, fields that are inside the droplet. This leads to the decay of the self-consistent field δ of the scalar fluctuation φ_f with the decay rate of the same order as predicted for the SM Higgs particle. Thus, roughly speaking, the decay width of the Wbgfms configuration will be of the order of a few MeV. Finally, only longer-lived particles are detected in the detector.

4.2. Transparency of the Uncharged bgfms Configuration to Electromagnetic Radiation. In Sec. 3, it was noted that the effective mass m_A of the electromagnetic self-field A inside the droplet of an electrically uncharged Wbgfms configuration is equal to zero. Although the electromagnetic self-field is totally absent in this bgfms configuration (see Sec. 3), zeroing of the effective mass and $\varrho_{fQ} = 0$ are important for the photons that are external ones (see Introduction). The reason is that the formal form of the equations of motion (77)–(79) is also true for the external gauge fields penetrating the discussed bgfms configuration. Thus, the Wbgfms configuration is transparent for the external electromagnetic radiation.

Now, let us suppose that the matter is extremely dense, as could happen in the mergers of neutron stars. Then the difference between the inward structure of the nucleon and the inward structure of the droplet of the Wbgfms configuration may be a supporting impulse to initiate the relativistic shock. That is, the abrupt transition of the neutron matter during the collapse of star mergers could cause the transition to matter of Wbgfms droplets, which are transparent to the gamma radiation that is produced within the gamma-ray bursts (GRB) explosion. This can lead to the appearance of an alternative source of energy that can help the gamma-ray burst [7]. This would also be the reason for the recently observed lack of correlations between gamma-ray bursts and the neutrino fluxes (present in the Standard Model [66]) and directed from them [67–70].

CONCLUSIONS

The aim of this paper was to examine homogeneous self-consistent ground state solutions in the CGSW model [1]. It is an effective one, as is the GSW model, which is its quantum counterpart. It is assumed that if the ground state of the configuration of the self-fields induced by extended (nonbosonic) charge fluctuations appears [2], then this forces us to describe the physical system inside its droplet in the manner of classical field theory.

Let us summarize the results presented in this paper. The discussed model is homogeneous on the level of one droplet (thus, the thin wall approach is

used). The homogeneous configurations of the gauge ground self-fields $W^{\pm}_{1,2}$, Z_0, and A_0 and the scalar field fluctuation φ_f in the presence of a spatially extended homogeneous basic fermionic fluctuation(s), that carries the nonzero charges, were examined. The ground fields penetrate the whole spatially extended fermionic fluctuation(s) and in their presence the electroweak force generates "the electroweak screening fluctuation of charges" according to Eqs. (19)–(22).

In general, we notice two physically different configurations of the fields. When a matter source has the charge density fluctuation $\varrho_{fQ\,\mathrm{SR}} \neq 0$, then classes* of the ground fields EWbgfms configurations (with $\vartheta \neq 0$ and $\delta \neq 0$) that are induced by this source exist (see Sec. 2). The mass (51) of a droplet of this configuration of field was determined for the value of the matter electric charge fluctuation equal to q_f (50). The EWbgfms configurations lie on the $M_{q_f}(\varrho_{fQ})$ curves (see Fig. 4, *a*) or equivalently on the $\mathcal{E}_{\mathrm{st}}(\varrho_{fQ\,\mathrm{SR}})$ curves only (see Fig. 3, *b*). For the particular value of p, the functions $M_{q_f}(\varrho_{fQ\,\mathrm{SR}})$, (51), and their minima $M^{\min}_{q_f}$ depend on λ (see Fig. 4, *a*).

Inside the droplet, both the appearance of the mass of the (non-self-consistently treated) wavy self-field $\tilde{A}_\mu$ and the modification of the masses of the wavy self-fields $\tilde{W}^{+}_{\mu}$–$\tilde{W}^{-}_{\mu}$, $\tilde{Z}_\mu$, and also the scalar fluctuation field φ_f are caused due to the existence of the self-consistent fields (see Subsec. 1.1) and the screening effect of the fluctuation of charges formulated by Eqs. (19)–(22). Then, the obtained masses are used in order to estimate the thin wall approximation range. A more complete description of the EWbgfms configurations, e.g., the dependence of the observed charge density fluctuation ϱ_{fQ} on $\varrho_{fQ\,\mathrm{SR}} \neq 0$ and the modification of the mixing angle Θ, (39), with a change of ϱ_{fQ} and the stability of the EWbgfms configurations is given in Sec. 2.

When the weak charge density fluctuation $\varrho_{fZ\,\mathrm{SR}} \neq 0$ (and $\varrho_{fQ\,\mathrm{SR}} = 0$), then the electrically uncharged, weakly charged Wbgfms configurations with $\vartheta = 0$ and $\delta \neq 0$, and the ground self-field $Z_0 = \zeta \neq 0$ can exist (see Sec. 3). The region of the stable (for the sake of the $W^{\pm}$ sector) Wbgfms configurations lies on and below the $\varrho_{fZ\,\mathrm{SR\,max}}(\lambda_{\max})$ boundary curve (see Fig. 7, *a*). For the particular value of i^3_f, (74), the function $\varrho_{fZ\,\mathrm{SR\,max}}(\lambda_{\max})$ gives the function $M^{\max}_{i^3_f}(\lambda_{\max})$, which divides the plane $\lambda \times M_{i^3_f}$ of all Wbgfms configurations into the stability and instability regions (see Fig. 7, *b*). A more complete description of the Wbgfms configurations can be found in Sec. 3.

Previously, in [1] it was found that for $\lambda = 1$ and $p = 2$ a shallow minimum of the mass of the EWbgfms configuration droplet equal to $M^{\min}_{q_f} \approx \pm q_f \cdot 66.7464$ GeV appears. At that time the expectation was that the ap-

*For $p \neq 0$, where examples are given in the Table. One bgfms droplet with certain values of quantum numbers does not convert (without decay or radiation) to another configuration of fields with different quantum numbers.

pearance of such bgfms configurations might be theoretically possible in the very dense microscopic objects that are created in heavy-ion collisions [21]. In the present paper in Sec. 4, the complete characteristics of two such bgfms configurations $s1_{q_f=2}$ and $s2_{q_f=2}$ were given. We only remind the reader that for the zero spin $s1_{q_f=2}$ state (realized for $\lambda \approx 0.0652$) the mass of the EWbgfms droplet equal to $M^{\min}_{q_f=2} \approx 126.67$ GeV was obtained. The physical realization of the other EWbgfms $s2_{q_f=2}$ state (at least as far as its mass is taken into account) is doubtful, as the fields configuration inside the droplet of its electrically neutral Wbgfms successor $s2_{i^3_f=\mp 1/2}$ is induced by one fermionic fluctuation only thus having a half spin value, which is less consistent with the observations reported in the LHC experiment [71–76]. As was previously only mentioned, the algebraic mean of the mass of the central solutions $s1$ and $s2$, i.e., 126.67 and 123.7 GeV, respectively, is equal to 125.185 GeV.

Thus, the remaining zero spin EWbgfms state $s1_{q_f=2}$ is the configuration in the minimum of the $M_{q_f}(r_{q_f})$ curve for $p = 2$, $q_f = 2$ and with $\lambda \approx 0.0652$ (see Fig. 4, *a*). It lies on the $M^{\min}_{q_f=2}(\lambda)$ curve at the point of its intersection with the boundary curve $M^{\max}_{i^3_f=\mp 1}(\lambda = \lambda_{\max} \approx 0.0652)$ (see Fig. 8, *a*). The intersection point is interpreted as the one that corresponds to the transition of the electrically charged EWbgfms configuration $s1_{q_f=2}$ to the electrically uncharged zero spin Wbgfms state $s1_{i^3_f=\mp 1}$, which has the mass $M^{\max}_{i^3_f=\mp 1} \approx 126.67$ GeV, as can be seen in Fig 8, *b*. In Sec. 4, it was argued that the configuration $s1_{i^3_f=\mp 1}$ corresponds to the LHC ~ 126.5 GeV zero spin state. This physically interesting solution, which is discussed in the present paper, has not been found before (see Fig. 8, *a*).

In this paper, it was also noted that for both the EWbgfms and Wbgfms configurations the nonzero charge fluctuations (fundamentally ϱ_{fY}) imply a nonzero value of the self-consistent field $\delta \neq 0$ of the scalar fluctuation φ_f (compare Notes in Sec. 2 below Eq. (46) and in Sec. 3 below Eq. (56)). Thus, in the more fundamental theory, the self-consistent field δ could be a secondary quantity. Because for both EWbgfms and Wbgfms configurations (for which $\varrho_{fY} \neq 0$), we find that the limit $\varrho_{fY} \to 0$ implies $\delta \to v$, thus a derivative meaning for the parameter v of the scalar fluctuation potential may also be suggested.

Finally, if Wbgfms state $s1_{i^3_f=\mp 1}$ is interpreted as the LHC ~ 126.5 GeV one, then this means that the value of $\lambda = \lambda_{\max} \approx 0.0652$, which is the constant parameter of the CGSW model, is a little bit bigger than the limiting stability value $\lambda^{\text{limit}} = g^2/(16 \cos^4 \Theta_W) \approx 0.0451$ (see Sec. 3 and Fig. 7, *a*, *b*). A bgfms state exists for $\lambda \approx 0.0652$ only (although other specific values of λ are possible in an extension of the model, see Eq. (75)). Therefore, a Wbgfms configuration of fields with $\varrho_{fZ\,\mathrm{SR}}$ bigger than $\varrho_{fZ\,\mathrm{SR\,max}} \approx 9.249 \cdot 10^6$ GeV^3 (which is the density for

$s1_{i_f^3=\mp 1}$ state, calculated in accordance with Eq. (72)) lies above the $s1_{i_f^3=\mp 1}$ state in the instability region (see Fig. 7) and is unstable in the $W^{\pm}$ sector. Therefore, as was suggested in [1], it radiates to the states with $\varrho_{fZ\,\mathrm{SR}} \leqslant \varrho_{fZ\,\mathrm{SR\,max}}$ or decays into stable particles, i.e., photons, leptons, hadrons, and neutrinos, as was described in Subsec. 4.1.

The nonlinear self-consistent classical field theory is inherently connected with the existence of the self-field [10–15, 19] coupled to the basic field (fluctuation). For example, in the perturbative QED the classical self-field of the electron fluctuation is completely absent and it comes back in via a separate quantized radiation field "photon by photon". Meanwhile, in the self-consistent classical field concept, the whole self-field is put in from the beginning. It is free of the idea of the quantum field theory vacuum (state) [77] and the virtual pair creation.

The self-field concept was previously used with great success in the Abelian case, e.g., in order to compute nonrelativistic Lamb shifts and spontaneous emission [22, 23], the Lamb shift (obtained iteratively) [20], spontaneous emission in cavities [24], and long-range Casimir–Polder van der Waals forces [25]. These analyses follow the work of Jaynes and Milonni [26–29] and the even earlier paper of Callen and Welton [78] on the fluctuation dissipation theorem, which showed that there is an intimate connection between vacuum fluctuations and the process of radiation reaction. The existence of one implies the existence of the other.

The linear Dirac equation alone with, e.g., the electron wave function in the presence of the (external to it) Coulomb field leads to wave mechanical solutions for the ground and excited states of the electron in an atom (see Introduction). The mathematics of the nonlinear Dirac equation for the basic field fluctuation which follows from the coupled Maxwell and linear Dirac equations for this fluctuation and its electromagnetic self-field is quite different. In general, the mathematics of the self-consistent field theory is interested in a proper set of partial differential equations, which are then solved self-consistently in such a way that all degrees of freedom are removed. What remains is one particular state of the system.

Remark. For example, the self-consistent solution of the couple: the Dirac equation and classical Maxwell equations, — will give a real photon, that is a "lump of electromagnetic substance" (without Fourier decomposition [6, 39], as is suggested from recent experiments [79]) as the reflection of the coupling to the Dirac equation. If we pull back from this particular solution forgetting about the primary Dirac equation, then what remains are not the classical Maxwell equations for the classical electromagnetic field but equations that act on the space of possible photonic states. QED with the field operator and the Fock space have to be the non-self-consistent reflection of this construction (if only the Fourier

decomposed frequencies of the light pulse represent actual optical frequencies, which have recently been questioned by light beam experiments [79]). Compare the self-consistent pair of Eqs. (55) and (56) with the non-self-consistent Eq. (76).

The merits of the thought that is behind this procedure is the self-consistency of the solution. The further we are from this precise self-consistent solution, the more numerous sets of differential equations remain to be solved, but the set of equations that are already solved determine the types of the equations which remain and the properties of the fields that are ruled by them. The self-field is small for atomic phenomena, and therefore the description of the basic field fluctuation via the linear Dirac equation may work approximately, which follows from the fact that the nonlinear terms are small and can be treated as perturbations. Nevertheless, the QED prevailed, mainly because of the success in the scattering phenomena.

Yet, the self-field is not always small and there is another region where the nonlinear terms dominate [14, 15]. The present paper reflects such a situation, since for the bgfms configuration of fields, the energy of the host fermionic fluctuation is assumed to be minute in comparison to the obtained mass of the bgfms droplet. Thus, the main theoretical subject of this paper was the self-consistent description of the configuration of electroweakly interacting self-fields that are induced by a charge density fluctuation(s) with the internal extended wave structure inside one droplet. Thus, the CGSW model is the type of "a source theory" that considers all self-fields and scalar field fluctuations as "derived" from the source of the fluctuations of charges. The quotation marks mean that the self-consistent fields are not absent — they are only self-consistently derived from the basic fluctuations fields to which they are coupled via the screening condition of the fluctuation of charges (19)–(22).

In the presented CGSW model of the bgfms configuration of fields induced by the basic matter field fluctuation(s), the droplet is like the whole particle. This is connected with the fact that (besides the fact that the energy of the fermionic fluctuation is ignored) any fermionic fluctuation which "stretches" the droplet is like a whole fermion. Thus, our droplet of the bgfms configuration is like "a parton". This is definitely not the most general case.

The indispensable need for the development of a more general approach is seen from the self-consistent model of the configuration of fields induced by the electronic charge fluctuation used in the Lamb shift explanation, where the energy of the electronic fluctuation is ignored (not to mention the ground and excited states of the electron, which are obtained in the anticipation by the formalism of the wave mechanics for the total electron wave function that is treated non-self-consistently). Therefore, let us assume that there is an object in which the fluctuation of the fermionic charge does not exist by itself but needs a globally extended fermionic charge of which it is the disturbance only. With such an approach, one is obliged to define and find the mass of

the configuration of fields induced by the globally extended charge together with its fluctuation(s) (extended globally or locally). In doing this, one should focus on neither the wave mechanics (or quantum mechanics) nor on the self-consistent field theory of fluctuations (or quantum field theory), but on the theory of the complete inner structure of one particle. Otherwise, the model gets into the composition of "a particle" from "partons", which is a kind of "planetarianism", and seemingly because of this, e.g., quantum chromodynamics (QCD) is the theory without final fundamental success [80], as was expressed in [81]: "... all spin parts [of the nucleon] have to add to 1/2 which is incredible in the light of the present day experiments. This may indicate that some underlying symmetries, unknown at present, are playing a role in forming the various contributing parts such that the final sum rule gives the fermion 1/2 value".

Both to recapitulate and go a little bit further, in order to describe the state of one particle (or even one droplet with a fluctuation) in a fully self-consistent way, the interaction of the self-fields with the globally extended charge and fluctuations inside this particle (possibly ruled by equations unknown at present) has to be considered simultaneously. Consequently, further analysis should describe a more realistic shape of the charge density of the extended matter source. Supposing that proper equations are known, this shape should follow, e.g., from the coupled Klein–Gordon–Maxwell (Yang–Mills) or Dirac–Maxwell (Yang–Mills) equations [82] and from Einstein's equations (or equations of an effective gravity theory of the Logunov type [83, 84]) as is required for the self-consistent models. Thus, to make the theory of one particle fully self-consistent, even a model of gravitation should be included [17]. Hence, a matter particle (similar to one droplet induced by matter fluctuations) seems to be, from the mathematical point of view, a self-consistent solution of all of the field equations involved in the description of the constituent fields inside this particle. Its interaction as a whole with the outer world is ruled by other models.

The presented electroweak CGWS model, although elaborated on for configurations of fields inside one particle that are induced by the basic matter fluctuations only, is the next step towards the self-field formalism [6, 30–37, 39] of the classical theory of one elementary particle. This particle is a materially extended entity with its own self-fields (e.g., electroweak, gravitational, etc.) coupled self-consistently to the basic fields inside it.

In [17] and in the present paper, it is suggested that the realization of such an analysis in the derivation of the characteristics of one particle is at hand.

Acknowledgements. This work has been supported by L. J. CH. This work has been also supported by the Department of Field Theory and Particle Physics, Institute of Physics, University of Silesia, and by the Modelling Research Institute, Katowice, Poland.

Appendix 1
QUANTUM NUMBERS IN THE CGSW MODEL

Some quantum numbers in the CGSW $SU_L(2) \times U_Y(1)$ model

	Weak isotopic charge I^3	Weak hypercharge Y	Electric charge Q $Q = I^3 + Y/2$	$p = 2Q/Y$
Leptonic fluctuations				
ν_{fL}	1/2	–1	0	0
ℓ_{fL}	–1/2	–1	–1	2
ℓ_{fR}	0	–2	–1	1
$\ell = e, \mu, \tau$				
Gauge self-fields				
W^+	1	0	1	
W^3	0	0	0	
W^-	–1	0	–1	
B	0	0	0	
Scalar fluctuations doublet Φ_f				
Φ_f^+	1/2	1	1	2
Φ_f^0	–1/2	1	0	0
Some source matter fluctuation configurations				
	–1/2	1	0	0
	–1	4	1	1/2
	0	2	1	1
	1/2	1	1	2
	3/2	1	2	4

Appendix 2
THE CGSW MODEL FIELD EQUATIONS WITH CONTINUOUS MATTER CURRENT DENSITY FLUCTUATIONS

From (1) the field equations for the Yang–Mills self-fields follow ($\Box = \partial_\nu \partial^\nu$), for B^μ:

$$-\Box B^\mu + \partial^\mu \partial_\nu B^\nu = \frac{1}{4} g g' \varphi_f^2 W^{3\mu} + \frac{1}{4} g'^2 \varphi_f^2 B^\mu - \frac{g'}{2} j_{f\,Y}^{\mu}, \tag{77}$$

for $W^{a\mu} (a = 1, 2)$:

$$-\Box W^{a\mu} + g \varepsilon_{abc} W^{b\nu} \partial_\nu W^{c\mu} = \\ = g^2 \left(\frac{1}{4} \varphi_f^2 W^{a\mu} - W_\nu^b W^{b\nu} W^{a\mu} + W^{a\nu} W_\nu^b W^{b\mu} \right) - g j_f^{a\mu}, \tag{78}$$

and for $W^{3\mu}$:

$$-\Box W^{3\mu} + g\varepsilon_{3bc}W^{b\nu}\partial_\nu W^{c\mu} = \frac{1}{4}g^2\varphi_f^2 W^{3\mu} - \frac{1}{4}gg'\varphi_f^2 B^\mu - \\ - g^2 W_\nu^b W^{b\nu} W^{3\mu} + g^2 W^{3\nu} W_\nu^b W^{b\mu} - g j_f^{3\mu}. \quad (79)$$

Here $j_{f\,Y}^{\mu}$ and $j_f^{a\mu}$ are the continuous matter current density fluctuations extended in space, which are given by the equations

$$j_{f\,Y}^{\mu} = \overline{L}_f \gamma^\mu Y L_f + \overline{R}_f \gamma^\mu Y R_f, \quad (80)$$

$$j_f^{a\mu} = \overline{L}_f \gamma^\mu \frac{\sigma^a}{2} L_f, \quad \text{where} \quad a = 1, 2, 3. \quad (81)$$

Similarly, the fluctuation φ_f of the scalar field satisfies

$$-\Box\varphi_f = \left(-\frac{1}{4}g^2 W_\nu^a W^{a\nu} - \frac{1}{4}g'^2 B_\nu B^\nu + \frac{1}{2}gg' W_\nu^3 B^\nu\right)\varphi_f - \\ - \lambda v^2 \varphi_f + \lambda\varphi_f^3 + \frac{m_{\ell_f}}{v}(\overline{\ell}_{fL}\ell_{fR} + \text{h.c.}). \quad (82)$$

To simplify the calculations, we neglect the mass m_{ℓ_f} of the fermionic fluctuation ℓ_f. It could be smaller than the mass of, e.g., electron. But if ℓ_f coincided with the lepton ℓ, e.g., electron, then it would enter with a relative strength equal to $m_{e_f}/v \sim 2.1 \cdot 10^{-6}$.

REFERENCES

1. *Syska J.* Boson Ground State Fields in the Classical Counterpart of the Electroweak Theory with Nonzero Charge Densities // Frontiers in Field Theory / Ed. Kovras O. New York: Nova Sci. Publ., 2005. Ch. 6. P. 125–154.
2. *Mańka R., Syska J.* Boson Condensations in the Glashow–Salam–Weinberg Electroweak Theory. (This paper is drastically reinterpreted by [1] and the current paper) // Phys. Rev. D. 1994. V. 49, No. 3. P. 1468–1478.
3. *Grössing G., Pascasio J. M., Schwabl H.* A Classical Explanation of Quantization // Found. Phys. 2011. V. 41. P. 1437–1453.
4. *Keppeler S.* Torus Quantization for Spinning Particles // Phys. Rev. Lett. 2002. V. 89. P. 210405.
5. *Syska J.* Frieden Wave-Function Representations via an Einstein–Podolsky–Rosen–Bohm Experiment // Phys. Rev. E. 2013. V. 88. P. 032130.
6. *Syska J.* Maximum Likelihood Method and Fisher's Information in Physics and Econophysics. http://el.us.edu.pl/ekonofizyka/images/f/f2/Fisher.pdf. Univ of Silesia, 2012 (in Polish); arXiv:1211.3674.

7. *Biesiada M., Syska J.* Boson Condensates in Electroweak Theory and Gamma-Ray Bursts // Physica Scripta. 1999. V. 59, No. 2. P. 95–97.

8. *Arbuzov B. A., Zaitsev I. V.* LHC Would-Be $\gamma\gamma$ Excess as a Nonperturbative Effect of the Electroweak Interaction // Phys. Rev. D. 2012. V. 85. P. 093001.

9. *Syska J.* Remarks on Self-Consistent Models of a Particle // Trends in Boson Research / Ed. A. V. Ling. New York: Nova Sci. Publ., 2006. Ch. 6. P. 163–181.

10. *Barut A. O.* Towards a Theory of Single Events in Spin Correlation Experiments // New Techniques and Ideas in Quantum Measurement Theory. Ann. N. Y. Acad. Sci. 1986. V. 480. P. 393–399; Explicit Calculations with a Hidden-Variable Spin Model (and references therein) // Quantum Mechanics versus Local Realism: The Einstein–Podolsky–Rosen Paradox / Ed. F. Selleri. New York: Plenum Press, 1988. Ch. 18. P. 433–446.

11. *Barut A. O.* Combining Relativity and Quantum Mechanics: Schrödinger's Interpretation of ψ // Found. Phys. 1988. V. 18. P. 95–105.

12. *Barut A. O.* Schrödinger's Interpretation of ψ as a Continuous Charge Distribution // Ann. Phys. Leipzig. 1988. V. 45. P. 31–36.

13. *Barut A. O.* The Revival of Schrödinger's Interpretation of Quantum Mechanics // Found. Phys. Lett. 1988. V. 1. P. 47–56.

14. *Barut A. O.* The Schrödinger and the Dirac Equation — Linear, Nonlinear and Integrodifferential // Geometrical and Algebraic Aspects of Nonlinear Field Theory / Eds.: S. De Filippo, M. Marinaro, G. Marmo, G. Vilasi. Amsterdam: Elsevier Sci. Publ. B. V.; North-Holland, 1989. P. 37–51.

15. *Barut A. O., Ünal N.* An Exactly Soluble Relativistic Quantum Two-Fermion Problem // J. Math. Phys. 1986. V. 27. P. 3055–3060.

16. *Syska J.* Self-Consistent Classical Fields in Field Theories. Ph. D. Thesis. Unpublished. Univ. of Silesia, 1995/1999.

17. *Syska J.* Kaluza–Klein Type Model for the Structure of the Neutral Particle-Like Solutions // Intern. J. Theor. Phys. 2010. V. 49, No. 9. P. 2131–2157; arXiv:0903.3003.

18. *Sakurai J. J.* Modern Quantum Mechanics. Revised Edition / Ed. S. F. Tuan. Addison–Wesley Publ. Comp., 1994.

19. *Barut A. O., Kraus J.* Nonperturbative Quantum Electrodynamics: The Lamb Shift // Found. Phys. 1983. V. 13, No. 2. P. 189–194.

20. *Barut A. O. et al.* Relativistic Theory of the Lamb Shift in Self-Field Quantum Electrodynamics // Phys. Rev. A. 1992. V. 45, No. 11. P. 7740–7745.

21. *Kartavenko V. G., Gridnev K. A., Greiner W.* On Evolution of the Density Fluctuation. GSI Scientific Report / Ed. U. Grundinger. Gesellschaft für Schwerionenforschung (GSI) in der Helmholtz-Gemeinschaft, 2003. P. 43.

22. *Barut A. O.* Quantum Electrodynamics Based on Self-Energy // Physica Scripta. 1988. V. T21. P. 18–21.

23. *Barut A. O., Salamin Y. I.* Relativistic Theory of Spontaneous Emission // Phys. Rev. A. 1988. V. 37, No. 7. P. 2284–2296.

24. *Barut A. O., Dowling J. P.* Quantum Electrodynamics Based on Self-Energy: Spontaneous Emission in Cavities // Phys. Rev. A. 1987. V. 36, No. 2. P. 649–654.

25. *Barut A. O., Dowling J. P.* Quantum Electrodynamics Based on Self-Energy, without Second Quantization: The Lamb Shift and Long-Range Casimir–Polder van der Waals Forces near Boundaries // Phys. Rev. A. 1987. V. 36, No. 6. P. 2550–2556.

26. *Jaynes E. T.* Is QED Necessary? // Proc. of the Second Rochester Conf. on Coherence and Quantum Optics / Eds.: L. Mandel, E. Wolf. New York: Plenum Press, 1966. P. 21–23.

27. *Jaynes E. T., Cummings F. W.* Comparison of Quantum and Semiclassical Radiation Theory with Application to the Beam Maser // Proc. IEEE. 1963. V. 51, No. 1. P. 89–109.

28. *Jaynes E. T.* Electrodynamics Today // Coherence and Quantum Optics IV / Eds.: L. Mandel, E. Wolf. New York: Plenum Press, 1978. P. 495–510.

29. *Milonni P. W.* Classical and Quantum Theories of Radiation // Foundations of Radiation Theory and Quantum Electrodynamics / Ed. A. O. Barut. New York: Plenum Press, 1980. P. 1–21.

30. *Frieden B. R., Soffer B. H.* Lagrangians of Physics and the Game of Fisher Information Transfer // Phys. Rev. E. 1995. V. 52. P. 2274–2286.

31. *Frieden B. R.* A Probability Law for the Fundamental Constants // Found. Phys. 1986. V. 16. P. 883–903.

32. *Frieden B. R. et al.* Schrödinger Link between Nonequilibrium Thermodynamics and Fisher Information // Phys. Rev. E. 2002. V. 66. P. 046128.

33. *Frieden B. R. et al.* Nonequilibrium Thermodynamics and Fisher Information: An Illustrative Example // Phys. Lett. A. 2002. V. 304. P. 73–78.

34. *Frieden B. R.* Science from Fisher Information: A Unification. Cambridge UK: Cambridge Univ. Press, 2004.

35. *Syska J., Szafron R.* Informational Criteria for the Field Theory Models Building. In preparation.

36. *Piotrowski E. W. et al.* The Method of the Likelihood and the Fisher Information in the Construction of Physical Models // Phys. Stat. Sol. B. 2009. V. 246, No. 5. P. 1033–1037.

37. *Syska J.* Fisher Information and Quantum Classical Field Theory: Classical Statistics Similarity // Phys. Stat. Sol. B. 2007. V. 244, No. 7. P. 2531–2537.

38. *Amari S., Nagaoka H.* Methods of Information Geometry // Translations of Mathematical Monographs. V. 191. Oxford: Oxford Univ. Press, 2000.

39. *Sladkowski J., Syska J.* Information Channel Capacity in the Field Theory Estimation // Phys. Lett. A. 2012. V. 377, No. 1–2. P. 18–26.

40. *Chatrchyan S. et al. (CMS Collab.).* Study of the Mass and Spin-Parity of the Higgs Boson Candidate via Its Decays to Z Boson Pairs // Phys. Rev. Lett. 2013. V. 110. P. 081803.

41. *The ATLAS Collab.* An Update of Combined Measurements of the New Higgs-Like Boson with High Mass Resolution Channels. ATLAS-CONF-2012-170. 2012.

42. *Beringer J. et al. (Particle Data Group).* Physical Constants (rev.). Electroweak Model and Constraints on New Physics // Phys. Rev. D. 2012. V. 86. P. 010001-107–010001-136.

43. *Santilli R. M.* // Hadron. J. 1978. V. 1. P. 223–423; 574–901; 1267.

44. *Santilli R. M.* Recent Theoretical and Experimental Evidence on the Apparent Synthesis of the Neutron from Protons and Electrons. JINR Commun. E4-93-352. Dubna, 1993 (Chinese J. Syst. Eng. & Electr. 1995. V. 6. P. 177–199).

45. *Ferrero A., Altschul B.* Radiatively Induced Lorentz and Gauge Symmetry Violation in Electrodynamics with Varying α // Phys. Rev. D. 2009. V. 80. P. 125010.

46. *Diaz J. S.* Overview of Lorentz Violation in Neutrinos // Proc. of the DPF-2011 Conf. 2011; arXiv:1109.4620.

47. *Peck S. K. et al.* New Limits on Local Lorentz Invariance in Mercury and Cesium // Phys. Rev. A. 2012. V. 86, No. 1. P. 012109.

48. *Barut A. O., Van Huele J. F.* Quantum Electrodynamics Based on Self-Energy: Lamb Shift and Spontaneous Emission without Field Quantization // Phys. Rev. A. 1985. V. 32. P. 3187–3195.

49. *Aitchison I. J. R., Hay A. J. G.* Gauge Theories in Particle Physics. 2nd Ed. Bristol; Philadelphia: Adam Hilger, 1989.

50. *Biondini S. et al.* Phenomenology of Excited Doubly Charged Heavy Leptons at LHC // Phys. Rev. D. 2012. V. 85, No. 9. P. 095018.

51. *CMS Collab.* Observation of a New Boson at a Mass of 125 GeV with the CMS Experiment at the LHC // Phys. Lett. B. 2012. V. 716. P. 30–61.

52. *CMS Collab.* A New Boson with a Mass of 125 GeV Observed with the CMS Experiment at the Large Hadron Collider // Science. 2012. V. 338. P. 1569–1575.

53. *ATLAS Collab.* A Particle Consistent with the Higgs Boson Observed with the ATLAS Detector at the Large Hadron Collider // Ibid. No. 6114. P. 1576–1582.

54. *Barger V., Ishida M., Keung W-Y.* Total Width of 125 GeV Higgs Boson // Phys. Rev. Lett. 2012. V. 108. P. 261801.

55. CMS Higgs Physics Results. Constraints on the Higgs Boson Width from Off-Shell Production and Decay to $ZZ \to 4l$ or $2l2\nu$. CMS PAS HIG-14-002. 2014. https://twiki.cern.ch/twiki/bin/view/CMSPublic/Hig14002TWiki.

56. *Bilenkii M. et al.* Trilinear Couplings among the Electroweak Vector Bosons and Their Determination at LEP2 // Nucl. Phys. B. 1993. V. 409. P. 22–68.

57. *Gounaris G. et al.* Analytic Expressions of Cross Sections, Asymmetries and W Density Matrices for $e^+e^- \to W^+W^-$ with General Three-Boson Couplings // Intern. J. Mod. Phys. A. 1993. V. 08, No. 19. P. 3285–3320.

58. *Fleischer J., Kolodziej K., Jegerlehner F.* Transverse versus Longitudinal Polarization Effects in $e^+e^- \to W^+W^-$ // Phys. Rev. D. 1994. V. 49, No. 5. P. 2174–2187.

59. *Bella G., Charlton D., Clarke P.* Triple Gauge Boson Parameters. OPAL Technical Note TN-492. 1997.

60. *CMS Collab.* Properties of the Observed Higgs-Like Resonance Decaying into Two Photons. CMS Physics Analysis Summary. CMS PAS HIG-13-016. 2013; http://cds.cern.ch/record/1558930/files/HIG-13-016-pas.pdf.

61. *CMS Collab.* Search for $t\bar{t}H$ Production in Events with $H \to \gamma\gamma$ at $\sqrt{s} = 8$ TeV Collisions. CMS PAS HIG-13-015. 2013.

62. *Chatrchyan S. et al. (CMS Collab.).* Measurement of the Properties of a Higgs Boson in the Four-Lepton Final State // Phys. Rev. D. 2014. V. 89. P. 092007 (P. 18; 26; 27); arXiv:1312.5353v3 (P. 24; 34; 36).

63. *CMS Collab.* Evidence for the Direct Decay of the 125 GeV Higgs Boson to Fermions (Figure 1 for $H \to \tau\tau$ (non-VH) (obs.)) // Nature Phys. 2014. V. 10. P. 557–560; https://twiki.cern.ch/twiki/bin/view/CMSPublic/Hig13033PubTWiki. 2014.

64. *Olive K. A. et al. (Particle Data Group).* The Review of Particle Physics (2015) // Chin. Phys. C. 2014. V. 38. P. 090001 (and 2015 update).

65. *Khalil S., Moretti S.* Can We Have Another Light ($\sim$ 145 GeV) Higgs Boson? arXiv:1510.05934.

66. *Syska J., Dajka J., Luczka J.* Interference Phenomenon and Geometric Phase for Dirac Neutrino in π^+ Decay // Phys. Rev. D. 2013. V. 87. P. 117302; arXiv:1309.7536.

67. *LoSecco J. M.* Search for Gamma-Ray-Burst Correlation with Neutrinos // Astrophys. J. 1994. V. 425, No. 1. P. 217–221.

68. *Abbasi R. et al. (IceCube Collab.).* Limits on Neutrino Emission from Gamma-Ray Bursts with the 40 String IceCube Detector // Phys. Rev. Lett. 2011. V. 106, No. 14. P. 141101.

69. *Taboada I.* A Review of Particle Astrophysics with IceCube // Mod. Phys. Lett. A. 2012. V. 27, No. 39. P. 1230042.

70. *IceCube Collab.* An Absence of Neutrinos Associated with Cosmic-Ray Acceleration in γ-Ray Bursts // Nature. 2012. V. 484. P. 351–354.

71. *Miller D. J.* Measuring the Spin of the Higgs Boson from Higgs-Strahlung Physics and Experiments with Future Linear e^+e^- Colliders // AIP Conf. Proc. 2000. V. 578. P. 222–225.

72. *Miller D. J. et al.* Measuring the Spin of the Higgs Boson? // Phys. Lett. B. 2001. V. 505. P. 149–154.

73. *Gao Y. et al.* Spin Determination of Single-Produced Resonances at Hadron Colliders // Phys. Rev. D. 2010. V. 81. P. 075022.

74. *Englert Ch. et al.* Higgs Quantum Numbers in Weak Boson Fusion // JHEP. 2013. V. 01. P. 148.

75. *Djouadi A. et al.* Probing the Spin-Parity of the Higgs Boson via Jet Kinematics in Vector Boson Fusion // Phys. Lett. B. 2013. V. 723. P. 307–313.

76. *Ellis J., Hwang D. S.* Does the "Higgs" Have Spin Zero? // JHEP. 2012. V. 09. P. 071.

77. *Nedelko S. N., Voronin V. E.* Domain Wall Network as QCD Vacuum and the Chromomagnetic Trap Formation under Extreme Conditions // Eur. Phys. J. A. 2015. V. 51. P. 45.

78. *Callen H. B., Welton T. A.* Irreversibility and Generalized Noise // Phys. Rev. 1951. V. 83, No. 1. P. 34–40.

79. *Roychoudhuri Ch.* The Nature of Light. What Is a Photon? / Eds.: Ch. Roychoudhuri, A. F. Kracklauer, K. Creath. Boca Raton: CRC Press, 2008. P. 363–377.

80. *Gross F., Ramalho G., Peña M. T.* Spin and Angular Momentum in the Nucleon // Phys. Rev. D. 2012. V. 85. P. 093006.

81. *Heyde K.* Basic Ideas and Concepts in Nuclear Physics. An Introductory Approach. 3rd Ed. IOP Publ. Ltd, 2004. P. 577.

82. *Mańka R., Bednarek I.* Nucleon and Meson Effective Masses in the Relativistic Mean-Field Theory // J. Phys. G: Nucl. Part. Phys. 2001. V. 27, No. 10. P. 1975–1986.

83. *Denisov V. I., Logunov A. A.* The Theory of Space-Time and Gravitation // Gravitation and Elementary Particle Physics. Physics Series / Ed. A. A. Logunov. M.: Mir, 1983. P. 14–130.

84. *Lämmerzahl C.* Testing Basic Laws of Gravitation — Are Our Postulates on Dynamics and Gravitation Supported by Experimental Evidence? // Mass and Motion in General Relativity / Eds.: L. Blanchet, A. Spallicci, B. Whiting. Springer, 2011. P. 25–65.